Genetic analysis of triplicated genes affecting sex-specific skeletal deficits in Down syndrome model mice

Kourtney Sloan[1], Kristina M. Piner[1], Pathum Randunu Nawarathna Kandedura Arachchige[2], Charles R. Goodlett[3], Yann Herault[4], Gayla R. Olbricht[2], Joseph M. Wallace[5], and Randall J. Roper[1,6]

[1]Department of Biology, Indiana University Indianapolis, IN, USA;

[2]Department of Mathematics and Statistics, Missouri University of Science and Technology, Rolla, MO, USA;

[3]Department of Psychology, Indiana University Indianapolis, IN, USA;

[4]Department of Translational Medicine and Neurogenetics, Université de Strasbourg, Centre National de la Recherche Scientifique, Institut National de la Sante et de la Recherche Medicale, Institut de Génétique et de Biologie Moléculaire et Cellulaire, Illkirch, France;

[5] Weldon School of Biomedical Engineering, Purdue University, Indianapolis, IN, USA;

[6]Corresponding Author

Randall J. Roper

rjroper@iu.edu

ORCID: 0000-0002-9860-6037

Key Words: Trisomy 21, appendicular skeleton, femur, micro-computed tomography, Ts66Yah, Ts65Dn, construct validity

Abstract

Down syndrome (DS) is caused by triplication of human chromosome 21 (Hsa21), resulting in skeletal insufficiency and altered postnatal bone development in individuals with DS. DS mouse models have shown similar deficits to humans with DS, mimicking differences between ages, sexes, and bone compartments. The historic mouse model, Ts65Dn, has provided much of the mechanistic insight behind these DS-related skeletal deficits, but there are concerns over its genetic construct validity. Ts65Dn mice have an additional 60 trisomic genes that are homologous to Hsa6. These genes, acting either directly or through interactions with trisomic, Hsa21-homologous or disomic genes, may produce phenotypes not related to DS; so, Ts66Yah mice were derived to remove these genes. After assessing individual densitometric and morphometric parameters in femurs, skeletal phenotypes were directly compared between male and female Ts65Dn and Ts66Yah mice at postnatal day (P) 36 and 6-weeks and between male mice at 16-weeks using multivariate principal components analyses on these parameters. These comparisons confirmed male Ts66Yah mice have trabecular and cortical deficits similar to male Ts65Dn mice at all ages. In contrast, female Ts66Yah mice lacked trabecular deficits evident in female Ts65Dn mice at P36, but both ages had similar cortical deficits. Copy number normalization of *Dyrk1a,* a trisomic, Hsa21-orthologous gene, failed to rescue deficits in male or improve trabecular bone in female Ts66Yah mice at P36 as observed in Ts65Dn mice. Thus, mechanisms behind trabecular phenotypes in both sexes of Ts66Yah mice likely differ from those of Ts65Dn mice. Overall, the trisomic, Hsa6-homologous genes in Ts65Dn mice may result in differences in trabecular phenotypes or mechanisms prior to 6 weeks but do not impact later trabecular or cortical phenotypes.

Introduction

Down syndrome (DS), occurring in about 1 in 800 live births (DE GRAAF *et al.* 2017), is caused by Trisomy 21 (Ts21) and is the most common aneuploidy, resulting in an extra full or partial human chromosome 21 (Hsa21). Ts21 has been known to affect many bodily systems, including the nervous, immune, respiratory, cardiovascular, and musculoskeletal (ANTONARAKIS *et al.* 2020). People with DS also have an increased likelihood to have several comorbidities associated with these systems, such as Alzheimer's disease, leukemias, obstructive sleep apnea, and osteoporosis. It is largely unknown if these phenotypes are caused by the dysregulation of some or all of the 200-300 protein-coding Hsa21 genes and/or the presence of a freely segregating, extra chromosome itself, no matter which genes are dysregulated (XING *et al.* 2023). The genetic mechanism, including which genes and how many genes are involved, may also vary between phenotypes and may result in a developmental and/or progeroid trajectory (MOYER *et al.* 2021).

All people with DS have musculoskeletal abnormalities that lead to the heightened risk of osteoporosis. Related to skeletal deficits, individuals with DS are predisposed to joint laxity, muscle hypotonia, and inflammatory arthritis starting early in life and degenerative osteoarthritis later in life (VAN ALLEN *et al.* 1999; HENDERSON *et al.* 2007; FOLEY AND KILLEEN 2019). Within the skeleton, smaller bones, including shortened femurs, have been noted in individuals with DS, suggesting there are developmental differences in addition to advanced aging (THOMAS AND ROPER 2021). People with DS compared to the general population reach peak bone mass 5-10 years earlier, shortening the period of bone growth, and further suggesting developmental differences are present in the musculoskeletal system (COSTA *et al.* 2018). This can result in low bone mineral density (BMD) at skeletal maturity, which is further exacerbated by BMD that decreases with age more so in individuals with DS than those without (CARFI *et al.* 2017; GARCIA HOYOS *et al.* 2019; TANG *et al.* 2019). The contribution of developmental differences and

premature aging to DS skeletal deficits may also vary by sex. Women with DS maintain similar bone mineral apparent density (BMAD) at the femoral neck as women without DS until their 40s, whereas men with DS only maintain similar BMAD as men without DS until their 30s (CARFI *et al.* 2017). These sex differences are also dependent on bone compartment. Men with DS over the age of 18 have lower integral (cortical + trabecular) volumetric bone mineral density (vBMD), trabecular vBMD, cortical vBMD, and cortical thickness in their femurs compared to men without DS, while women with DS only had lowered cortical parameters compared to women without DS (GARCIA HOYOS *et al.* 2019). Males with DS over the age of 15 had lower integral and trabecular vBMD than females with DS but no differences in cortical vBMD (COSTA *et al.* 2021). Both advanced age and female sex are factors for increased fractures in individuals with DS (KRIEG *et al.* 2024).

To investigate Ts21 gene-phenotype relationships, multiple DS mouse models with varying content and transmission of triplicated genes are utilized due to differences between mouse and human genetics. The first viable mouse model of DS was the Ts(17^{16})65Dn (Ts65Dn), which has a freely segregating minichromosome that is trisomic for ~50% of Hsa21 orthologous genes found on mouse chromosome (Mmu)16 from *Mir155* to *Zbtb21* (STURGEON AND GARDINER 2011; DUCHON *et al.* 2022). Ts65Dn mice have been extensively studied and show many DS-like phenotypic similarities to humans with DS, including in the skeletal system. The cartilage template and primary ossification center of Ts65Dn embryos indicate deficits arise from abnormalities in mineralization rather than the building of the cartilage template (BLAZEK *et al.* 2015b). In postnatal studies, male Ts65Dn mice have cortical deficits as early as postnatal day (P)12 while trabecular deficits do not persist until P30 (LACOMBE *et al.* 2024). Trabecular and cortical deficits have been reported in male Ts65Dn mice at P36, P42 (6 weeks), 8 weeks, 12 weeks (3 months), 16 weeks, and 24 months (BLAZEK *et al.* 2011; FOWLER *et al.* 2012; WILLIAMS *et al.* 2018; SHERMAN *et al.* 2022; LACOMBE *et al.* 2024). Less is known about female

Ts65Dn mice, but current findings suggest trabecular and cortical deficits are apparent at P30, subsequently normalize and then are found again at P42; no later ages have been investigated (THOMAS *et al.* 2021; LACOMBE *et al.* 2024).

The Hsa21 gene *dual specificity tyrosine phosphorylation-regulated kinase 1A* (*DYRK1A*) has been linked to altered skeletal development, with a singular effect on trabecular skeletal deficits in male mice, and interactive effects on cortical bone (ARRON *et al.* 2006; LEE *et al.* 2009; EGUSA *et al.* 2011; SLOAN *et al.* 2023). These studies suggested that reducing *Dyrk1a* copy number or its kinase activity in male Ts65Dn mice could rescue some skeletal deficits. The timing of the expression of *Dyrk1a* copy number reduction is crucial to its therapeutic effects: normalization of *Dyrk1a* copy number through breeding with a *Dyrk1a* haploinsufficiency model (*Dyrk1a*^{tm1Mla} or *Dyrk1a*$^{+/-}$) does not rescue skeletal deficits in embryonic Ts65Dn mice, but improves or rescues some skeletal deficits postnatally (P36-P42)(BLAZEK *et al.* 2015a; BLAZEK *et al.* 2015b; LACOMBE *et al.* 2024). Although, these improvements or rescues of skeletal phenotypes are limited to male mice only, as female mice are not affected by *Dyrk1a* copy number normalization at the same age (LACOMBE *et al.* 2024). Additionally, genetic reduction of *DYRK1A* in euploid individuals leads to skeletal deficits associated with DYRK1A syndrome (OTTE AND ROPER 2024).

Reducing DYRK1A kinase activity in Ts65Dn mice has been hypothesized to correct skeletal abnormalities. Epigallocatechin-3-gallate (EGCG), the main catechin found in green tea extract, and Silmitasertib, also known as CX-4945, both have an affinity for the ATP-binding site of DYRK1A that may reduce DYRK1A activity and been shown to have minimal or no improvement, or worsen cortical bone in Ts65Dn mice depending on dosage, timing of treatment based on DYRK1A expression, or length of treatment time (GOODLETT *et al.* 2020; JAMAL *et al.* 2022; LACOMBE *et al.* 2024). Leucettinib-21 is a second-generation of Leucettamine B analog that also binds to the DYRK1A ATP-binding pocket (LINDBERG *et al.* 2023), but is more

potent for DYRK1A (IC_{50} = 2.4 nM) than EGCG (491 nM) or CX-4945 (6.8 nM) (KIM *et al.* 2016; LINDBERG *et al.* 2023). A low-dose, 10-day treatment of Leucettinib-21 was shown to improve memory based on the novel object recognition test in adult male Ts65Dn mice (LINDBERG *et al.* 2023), and a 9-day prenatal treatment of 30mg/kg/day partially rescued congenital heart defects in Dp1Tyb embryos (LANA-ELOLA *et al.* 2024); however, this inhibitor has not been tested on other DS phenotypes.

In addition to Hsa21 homologs, Ts65Dn mice also contain a triplication of ~60 trisomic genes (~35 protein-coding) located on the Mmu17 centromeric region from *Scaf8* to *Pde10a* that are orthologous to Hsa6, rather than Hsa21 (DUCHON *et al.* 2011; REINHOLDT *et al.* 2011). It is unknown if or how much these non-orthologous trisomic genes play a role in observed DS-associated phenotypes, and the impact of these extra genes, either collectively or individually, on these phenotypes. To test the hypothesis that triplicated non-Hsa21 genes affect DS-associated traits, theTs66Yah mouse model was developed using CRISPR/Cas9 to remove the Mmu17 centromeric region from Ts65Dn mice (DUCHON *et al.* 2022). The resultant Ts66Yah (Ts(17^{16})66Yah) mice have been thus far characterized for craniofacial, behavior, morphological and molecular brain , and growth phenotypes from late embryos to almost middle age, all indicating Ts66Yah mice exhibit DS-associated phenotypes (DUCHON *et al.* 2022; GUEDJ *et al.* 2023; ADAMS *et al.* 2024; LANZILLOTTA *et al.* 2024). However, skeletal phenotypes of long bones in Ts66Yah mice have not been characterized or compared to those of Ts65Dn mice before this analysis.

To test the hypothesis that the *Scaf8* to *Pde10a* non-Hsa21 homologous region contributes to long bone skeletal abnormalities observed in Ts65Dn mice, the femoral structure of Ts66Yah and euploid littermate mice was characterized at 6-, 9-, and 16 weeks of age. Additionally, the influence of trisomic *Dyrk1a* on skeletal deficits was tested in Ts66Yah mice to understand if trisomic *Dyrk1a* was interacting with non-Hsa21 orthologous trisomic genes to

affect skeletal appendicular skeletal traits. The results from Ts66Yah mice were compared to those previously obtained from Ts65Dn mice.

Methods

Animals

Ts(17^{16})66Yah (Ts66Yah) mice were obtained from the French National Centre for Scientific Research (CNRS) courtesy of Dr. Yann Herault and have been described previously (DUCHON *et al.* 2022). Briefly, the Ts66Yah founder was generated using CRISPR/Cas9 technology in fertilized embryos obtained via *in vitro* fertilization between Ts(17^{16})65Dn/J (Ts65Dn; Jackson Laboratory strain #001924) sperm and B6C3BF1 oocytes. The founder was selected based on its possession of the expected deletion of the *Scaf8-Pde10a* region and new, proper junction of the minichromosome between the mouse chromosome (Mmu) 17 centromere and the *Mir155-Zbtb21* region of Mmu16. The founder mouse was mosaic, containing both the Ts65Dn minichromosome and Ts66Yah minichromosome, but the F1 generation, obtained from breeding with C57BL/6NCrl females, only contained the Ts66Yah minichromosome. These mice were backcrossed at least 10 times to F1 hybrids of C56BL/6NCrl and C3H/HeN congenic line for the BALB/c allele at the *Pde6b* locus (B6C3BF1). Subsequently, three female Ts66Yah mice were transferred to the Indiana University (IU) Indianapolis Science Animal Resource Center.

The IU Indianapolis Ts66Yah colony was maintained by breeding female Ts66Yah mice to male B6C3F1 mice obtained through crossing C57BL/6J (Jackson Laboratory strain #000664) and C3H/HeJ mice that carry retinal degeneration allele *Pde6b*^{rd1} (Jackson Laboratory strain #000659). For the reduction of *Dyrk1a* copy number experiment, female Ts66Yah mice were bred to male *Dyrk1a* heterozygous mutant (*Dyrk1a*^{tm1Mla} or *Dyrk1a*$^{+/-}$) mice (FOTAKI *et al.* 2002) to yield four potential offspring genotypes: euploid animals with homozygous wildtype *Dyrk1a* (euploid control with two functional copies of *Dyrk1a* [euploid]), euploid animals with heterozygous mutant *Dyrk1a* (euploid with one functional copy of *Dyrk1a* [euploid,*Dyrk1a*$^{+/-}$]), trisomic (Ts66Yah) animals with homozygous wildtype *Dyrk1a* (trisomic animals with three functional copies of *Dyrk1a* [Ts66Yah]), and trisomic (Ts66Yah) animals with heterozygous mutant *Dyrk1a* (trisomic animals with two functional copies of *Dyrk1a* [Ts66Yah,*Dyrk1a*$^{+/+/-}$]).

These *Dyrk1a*^{tm1Mla} mice are maintained by breeding with a B6C3F1 mouse, like the Ts66Yah mice, in our colony.

Ts66Yah mice were genotyped by PCR using the following primers to amplify the minichromosome breakpoint between the mouse chromosome (Mmu) 17 centromere and Mmu16 genes (*Mir155* to *Zbtb21*) (DUCHON *et al.* 2022): wt/dw TCTAGGATCAGTGGGACTTTTGT, wt-tg_up GGAAATATCGCACTTCACCAA, and tg_dw CATGGGTCTGTGTGGTTTTCT. *Dyrk1a* heterozygous mutants were genotyped by PCR using the following primers to amplify a segment of the neomycin cassette and exon 6/intron region 6-7 of *Dyrk1a* (FOTAKI *et al.* 2002): Dyrk1a Neo P1 ATTCGCAGCGCATCGCCTTCTATCGCC and Dyrk1a P3 CGTGATGAGCCCTTACCTATG.

All animals are weaned around postnatal day (P) 21 and housed in cages of 1-5 mice of mixed genotype with a nestlet for enrichment and access to food and water *ad libitum*. Two male Ts66Yah animals out of 183 total Ts66Yah animals allocated were removed from the study due to the presence of hydrocephalus at time of detection. All animal use and protocols were approved by the Institutional Animal Care & Use Committee (IACUC) at the IU Indianapolis School of Science (SC338R) and adhered to the requirements in the NIH Guide for the Care and Use of Laboratory Animals.

Leucettinib-21 (L21) treatment

Leucettinib-21 (L21) solution was made weekly by suspending 2mg of L21 in 1mL of the vehicle, 0.5% weight by volume carboxymethyl cellulose (CMC). The 2mg/mL L21 solution was diluted to 0.05mg/mL L21 working solution, which was stored at -20°C. Using the 0.05mg/mL L21 solution, each animal was weighed and treated daily (0.5mg/kg) via oral gavage from P21 until P35. Animals were euthanized after recording body weight on P36. Cohorts consisting of

one to three litters were alternated between vehicle and L21 treatment. If a cohort contained multiple litters, each litter was born within 1-3 days of each other.

Bone storage and micro-computed tomography (µCT) analysis

Right femurs were wrapped in 1x phosphate buffered saline (PBS)-soaked gauze and stored at -20°C until scanning. Six-, nine-, and sixteen-week-old Ts66Yah femurs were wrapped in parafilm to maintain hydration and single-scanned using a SkyScan 1172 µCT system (Bruker, Kontich, Belgium) with the following parameters: 60kV, 167uA, 885ms, 10-micron voxel size, Al 0.5mm filter, 0.7º rotation step and frame averaging of two. Two hydroxyapatite phantoms (0.25 and 0.75g/cm^3 CaHA) were used to calibrate bone mineral density for each scanning session.

Due to irreparable damage to the SkyScan 1172 µCT system, femurs from P36 mice were wrapped in parafilm and group-scanned (KOHLER *et al.* 2021) using a SkyScan 1272 µCT system (Bruker, Kontich, Belgium) with the following parameters: 70kV, 142uA, 1265ms, 10-micron voxel size, Al 0.5mm filter, 0.7º rotation step and frame averaging of two. Two hydroxyapatite phantoms (0.3 and 1.25g/cm^3 CaHA) were used to calibrate bone mineral density for each scanning session. No unstandardized comparisons were made between scans from different µCT systems.

All scans were reconstructed using NRecon with the following settings: ring artifact reduction 5, beam-hardening correction 20%, dynamic image (attenuation coefficient) boundaries 0.00 and 0.11. Reconstructed scans were rotated so the anterior surface of the distal growth plate faces right in the transaxial view for all bones. Using CTAnalyzer (CTAn), the trabecular region of interest (ROI) was defined as a 1mm section extending proximally from the end of the distal growth plate and isolated from the cortical bone. The cortical ROI was defined as a 1mm (6-, 9-, and 16-week-old mice) or 0.65mm (P36 mice) section extending distally from

the beginning of the third trochanter. Trabecular bone parameters, including bone mineral density (BMD), bone volume fraction (BV/TV), trabecular thickness (Tb.Th), trabecular separation (Tb.Sp), and trabecular number (Tb.N), were calculated using internal CTAn functions. Cortical bone parameters, including total cross-sectional area (Tt.Ar), marrow area (Ma.Ar), cortical bone area (Ct.Ar), cortical bone area fraction (Ct.Ar/Tt.Ar), cortical thickness (Ct.Th), periosteal perimeter (Ps.Pm), endocortical perimeter (Ec.Pm), maximum and minimum moment of inertia (I_{max} and I_{min}) for P36 bones, and cortical tissue mineral density (Ct.TMD), were calculated using a custom MATLAB code (BERMAN *et al.* 2015; STRINGER *et al.* 2017a).

Mechanical testing

Mechanical properties were determined as described previously (THOMAS *et al.* 2020). Briefly, 3-point femur bend was performed after µCT analysis of 6-, 9-, and 16-week-old right femurs using a TA ElectroForce 5500 testing machine while bones were hydrated using PBS (Eden Prairie, MN, USA). Right femurs were tested using a 5-, 6-, or 7mm support span (6, 9, and 16 weeks, respectively) in the anterior-posterior direction with the posterior surface in compression. A 10lb load was utilized for 6- and 9-week-old femurs, and a 50lb load was utilized for 16-week-old femurs. All bones were preloaded (0.2-0.4 N) to establish contact with the loading point located at the midshaft, then testing occurred at 0.025mm/sec to failure. The 0.2% offset method was utilized on the slope of the linear portion of the stress-strain curve to find the yield point. The ultimate point was determined as the maximum force reached, while the failure point was determined as where the bone broke. Two 6-week-old female euploid femurs were excluded from analysis due to not reaching a failure point before maximum displacement at 3.5mm. The following whole bone (extrinsic) parameters were reported from the force-displacement curve: yield and ultimate force, displacement and work to yield, postyield displacement and work, total displacement and work, and stiffness. Cortical geometry from µCT analysis was utilized to normalize the stress-strain curve from the force-displacement curve.

The following tissue-estimate (intrinsic) properties were reported from the stress-strain curve: yield and ultimate stress, strain to yield, total strain, modulus, resilience, and toughness.

Comparison between Ts65Dn and Ts66Yah mice

The trabecular and cortical bone parameter values of each animal were standardized using the mean and standard deviation of all within each mouse model (Equation 1). This was performed separately for each sex and age. Six-week-old euploid and Ts65Dn data came from a subset of data presented in (THOMAS *et al.* 2021), only including euploid littermates and Ts65Dn mice lacking OSX-cre, whereas 16-week-old euploid and Ts65Dn trabecular data came from (BLAZEK *et al.* 2011). The P36 euploid and Ts65Dn data came from (LACOMBE *et al.* 2024).

$$BMD_{Ts65Dn(standardized)} = \frac{BMD_{Ts65Dn} - Mean(BMD_{Ts65Dn})}{SD(BMD_{Ts65Dn})}$$

$$BMD_{Ts66Yah(standardized)} = \frac{BMD_{Ts66Yah} - Mean(BMD_{Ts66Yah})}{SD(BMD_{Ts66Yah})}$$

Equation 1: Example of how each parameter was standardized within mouse model separately for each sex and age. The BMD parameter is shown for illustration.

Principal components analysis (PCA) was performed on standardized µCT data of Ts65Dn mice, Ts66Yah mice, and each of their respective euploid littermate controls, separately for each sex, age, and bone compartment. Another PCA was performed on standardized µCT data of trisomic Ts65Dn mice, Ts66Yah mice, and *Dyrk1a* copy number reduction mice of both models, separately for each sex and bone compartment. The principal component 1 (PC1) loading for each parameter was multiplied by the animal's standardized value. Then, the sum of these transformations was calculated to produce a single value to represent the animal's trabecular or cortical bone, which will be referred to as the trabecular or cortical composite score (Equation 2, 3).

$$\mathrm{TB}composite = (PC1_{BMD} \times BMD) + (PC1_{BVTV} \times BVTV) + (PC1_{Tb.Th} \times Tb.Th) + (PC1_{Tb.Sp} \times Tb.Sp) + (PC1_{Tb.N} \times Tb.N)$$

Equation 2: Calculation performed for each animal to find the trabecular composite score using standardized trabecular parameters. For illustration, $PC1_{BMD}$ represents the loading on PC1 for the BMD parameter.

$$\mathrm{CT}composite = (PC1_{Tt.Ar} \times Tt.Ar) + (PC1_{Ma.Ar} \times Ma.Ar) + (PC1_{Ct.Ar} \times Ct.Ar) + (PC1_{Ct.Th} \times Ct.Th) + (PC1_{Ps.Pm} \times Ps.Pm) + (PC1_{Ec.Pm} \times Ec.Pm) + (PC1_{Ct.TMD} \times Ct.TMD)$$

Equation 3: Calculation performed for each animal to find the cortical composite score using standardized cortical parameters. For illustration, $PC1_{Tt.Ar}$ represents the loading on PC1 for the Tt.Ar parameter.

Statistical analysis

Chi-squared goodness of fit tests were performed using Microsoft Excel to determine differences between expected Mendelian and observed genotype ratios for total counts of pre- and post-weaned offspring of Ts66Yah × B6C3F1 and Ts66Yah × *Dyrk1a*$^{+/-}$ breeding schemes. Correlational analyses of body weight and femur length at P36 in euploid and Ts66Yah mice treated with vehicle and L21 were performed in Microsoft Excel separately for each sex using Pearson correlation coefficient and coefficient of determination from linear regression. Significance of these correlations were determined by two-tailed Student's t-distribution (α = 0.05). Trabecular and cortical composite scores generated from the PCAs were utilized as responses in a two-way ANOVA with mouse model (Ts65Dn vs. Ts66Yah) and genotype (euploid vs. trisomic) or *Dyrk1a* copy number (2 vs. 3) as between subject main effect factors, along with their interaction. When the interaction was significant, *post hoc* analyses between genotypes or *Dyrk1a* copy number within mouse model were performed with Bonferroni correction. Type III Sum of Squares were utilized for testing each factor due to differing numbers of mice per group. PCA and the two-way ANOVAs of composite scores were performed using R version 4.3.0. Remaining statistical analyses were performed using IBM SPSS Statistics (v29.0.1.0). The Shapiro-Wilk test (α = 0.05) was used to assess normality. In cases where the

data were non-normal, data were log-transformed and assessed again. The assumption of equal variances was assessed using Levene's test ($\alpha = 0.05$).

For 6-, 9-, and 16-week-old Ts66Yah trabecular and cortical μCT data, two-way ANOVAs were performed with genotype and age as between subject factors along with their interaction to assess growth. Due to known differences in male and female bone development, these were performed separately for each sex (SEEMAN 2003; ALSWAT 2017). For all 6-, 9-, and 16-week-old data, two-way ANOVAs with sex and genotype as between-subject factors were performed separately for each age. Sex-stratified *a priori* one-tailed t-tests were performed in the cases of significant genotype or sex effects but no interaction due to previous DS research showing deficits only appearing after analyzing sexes separately (LAMANTIA *et al.* 2024).

For the P36 germline reduction of *Dyrk1a* experiments, sex-stratified one-way ANOVAs were performed. For P36 L21 treatment change in weight, femur length, and μCT data, two-way ANOVAs with treatment and genotype as between-subject factors was performed separately for each sex. Additionally, for the P36 L21 treatment groups, a repeated measures ANOVA was performed in each sex for body weight using genotype and treatment as between subject factors and postnatal day as the within subject factor. Sphericity was assessed using Mauchly's test, and the Greenhouse-Geisser test was utilized to detect significant effects and interactions due to significant Mauchly's tests. Pairwise comparisons with a Bonferroni adjustment were utilized in cases where the within subject effect or interactions involving the within subject effect were significant.

P values generated from μCT and mechanical parameter ANOVAs were adjusted using the Benjamini-Hochberg FDR method for trabecular, cortical, extrinsic and intrinsic parameters independently (AN *et al.* 2013). A significant finding was defined as an unadjusted $p < 0.05$ in the case of body weight, femur length, and composite score data or an adjusted $p < 0.05$ in the case of μCT and mechanical parameters. Then, in cases where both Levene's test and the

adjusted ANOVA p value were significant ($p < 0.05$), the data were re-assessed by Welch's F statistic to confirm significance. If data were not significant during re-assessment, the parameter was not reported as significant. Finally, in cases where a significant interaction occurred between two between-subject factors, Tukey's or Games-Howell *post hoc* analysis ($\alpha = 0.05$) were used depending on Levene's test result.

Results

Higher rate of trisomy in Ts66Yah animals

The Ts66Yah x B6C3F1 breeding scheme has yielded 114 litters with an average litter size of 4-5 mice in our laboratory (Supplemental Table 1). The transmission of trisomy was 44% between P6 and P10 and at weaning, which is similar to that reported in another lab for the first year of breeding on a similar background (44%) but higher than their 6-year total (33%) (Duchon *et al.* 2022). Compared to Ts65Dn mice, this rate is also higher than previously reported transmission at weaning (~34%) (MOORE 2006; ROPER *et al.* 2006). The transmission rate at weaning was similar in both sexes when averaged across the years, but there were varying rates throughout the colony's time.

Ts66Yah mice were also bred with *Dyrk1a*$^{+/-}$ mice, yielding 26 litters with an average litter size of 5-6 mice (Supplemental Table 2). The transmission of trisomy was 57% between P6 and P10 and 58% at weaning. When broken down into the four possible genotypes, fewer euploid,*Dyrk1a*$^{+/-}$ and Ts66Yah mice were found between P6 and P10 while more Ts66Yah,*Dyrk1a*$^{+/+/-}$ mice were present than expected. This was the case in both male and female mice at weaning.

Skeletal phenotypes vary by age and sex in post-pubertal Ts66Yah mice

Appendicular skeletal phenotypes of Ts66Yah mice were evaluated after sexual maturity during skeletal accrual (6 and 9 weeks) and around skeletal maturity (16 weeks) as done for Ts65Dn and other DS mouse models. As male and female Ts66Yah and euploid littermates increased in age, both body weight and femur length increased (Supplemental Figure 1A-B). At 6-weeks-old, while there was an interaction of sex and genotype for body weight, *post hoc* analysis only showed sex differences in both genotypes and no differences between genotypes

of either sex (Supplemental Figure 1C). A significant sex effect was detected for femur length at 6 weeks of age, where male mice had longer femurs than female mice (Supplemental Figure 1D). The sex difference in femur length was not detected at 9-weeks-old, but a sex difference was still present for body weight, where male mice weighed more than female mice (Supplemental Figure 1C-D). By 16 weeks of age, both body weight and femur length had an effect of sex similar to that of 6-week-old mice (Supplemental Figure 1C-D). Sex-stratified one-tailed t-tests revealed significantly shorter femurs in male, but not female, 6- and 16-week-old Ts66Yah mice compared to their euploid littermates. Additionally, 9-week-old female Ts66Yah mice weighed more than female euploid mice, while males were unaffected.

As expected, trabecular bone parameters were affected by age (Figure 1B-F). Male and female 6-week-old mice had greater bone volume fraction (BV/TV) compared to 16-week-old mice and more trabeculae (Tb.N) compared to 9- and 16-week-old mice (Figure 1C,F). Male and female 9-week-old mice also had more trabeculae (Tb.N) than 16-week-old mice. Male and female 16-week-old mice had the greatest trabecular spacing (Tb.Sp), but only female mice had greater trabecular thickness (Tb.Th) at 9 and 16 weeks compared to 6 weeks (Figure 1D-E). No significant genotype × age interactions were detected.

There were no genotype effects observed for 6- or 16-week-old Ts66Yah mice, but at 9-weeks-old, Ts66Yah mice had lower Tb.Th compared to euploid littermates (Figure 1I). There was an effect of sex for all parameters at 6-weeks-old, where male mice had greater BMD, BV/TV, Tb.Th, Tb.N and lower Tb.Sp compared to female mice (Figure 1G-K). Similar changes for trabecular phenotypes were observed for 9- and 16-week-old mice apart from no significant difference in Tb.Th.

Sex-stratified one-tailed t-tests in 6-week-old mice showed male Ts66Yah mice had reduced BMD, BV/TV, Tb.Th and increased Tb.Sp compared to male euploid littermates. At 9 weeks, only trabecular thickness was significantly decreased in male Ts66Yah mice. By 16

weeks, BMD, BV/TV, and Tb.N were significantly decreased in male Ts66Yah mice. At all three timepoints, there were no significant trabecular differences between female euploid and Ts66Yah mice.

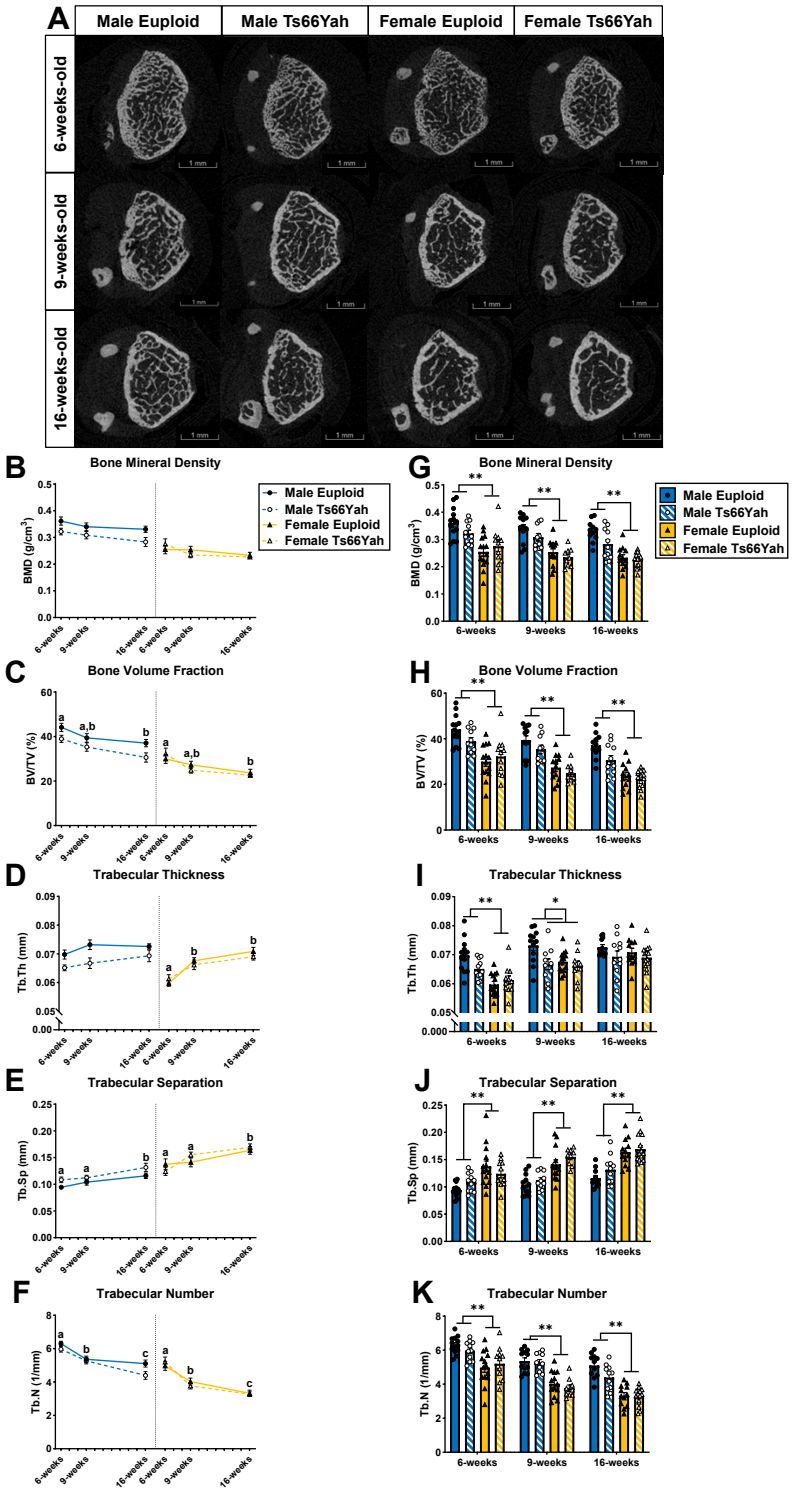

Figure 1: **Trabecular bone parameters for 6-, 9-, and 16-week-old Ts66Yah mice. A)** Representative images of trabecular bone taken halfway through the 1mm trabecular region as determined by finding the animal with the closest average distance away from the mean of each trabecular parameter. **B-F)** Data are mean ± SEM. Different letters indicate $p < 0.05$ between ages as determined by two-way ANOVA and

Tukey or Games-Howell *post hoc* analysis. **G-K)** Data are mean ± SEM. Different letters indicate significant differences between groups as determined by Tukey or Games-Howell *post hoc* analysis of significant genotype × sex interaction. Asterisks indicate a sex or genotype effect as determined by two-way ANOVA. * $p < 0.05$, ** $p < 0.01$. 6 weeks: male euploid (n = 13), male Ts66Yah (n = 11), female euploid (n = 14), female Ts66Yah (n = 11); 9 weeks: male euploid (n = 12), male Ts66Yah (n = 10), female euploid (n = 13), female Ts66Yah (n = 9); 16 weeks: male euploid (n = 11), male Ts66Yah (n = 11), female euploid (n = 12), female Ts66Yah (n = 15).

As expected, most cortical bone parameters increased with age while endocortical perimeter (Ec.Pm) and marrow area (Ma.Ar) decreased with age in female mice likely due to endocortical apposition, lack of osteoclast resorption, or a combination of these factors (Figure 2). Male and female 6-week-old mice had a smaller total cortical cross-sectional area (Tt.Ar) and periosteal perimeter (Ps.Pm) compared to 9- and 16-week-old mice (Figure 2A,F). Male mice also increased Ps.Pm from 9 to 16 weeks. Both 6- and 9-week-old female mice had a greater Ma.Ar and Ec.Pm compared to 16-week-old female mice (Figure 2B,G). Cortical area (Ct.Ar), cortical bone area fraction (Ct.Ar/Tt.Ar), cortical thickness (Ct.Th), and cortical tissue mineral density (Ct.TMD) increased at each age measured for both sexes (Figure 2C-E,H). No significant genotype × age interactions were detected.

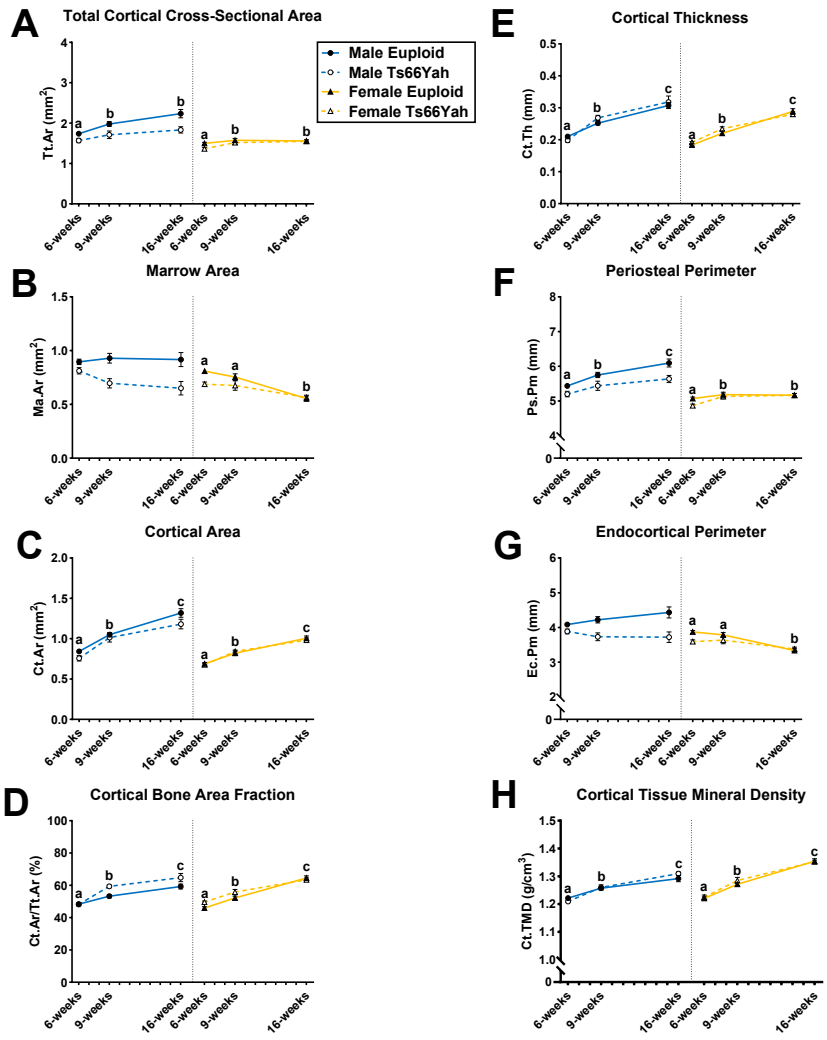

Figure 2: **Cortical bone growth curves for 6-, 9-, and 16-week-old Ts66Yah mice.** Data are mean ± SEM. Different letters indicate $p < 0.05$ between ages as determined by two-way ANOVA and Tukey or Games-Howell *post hoc* analysis. 6 weeks: male euploid (n = 13), male Ts66Yah (n = 11), female euploid (n = 14), female Ts66Yah (n = 11); 9 weeks: male euploid (n = 12), male Ts66Yah (n = 10), female euploid (n = 13), female Ts66Yah (n = 9); 16 weeks: male euploid (n = 11), male Ts66Yah (n = 11), female euploid (n = 12), female Ts66Yah (n = 15).

Six-week-old Ts66Yah mice were significantly lower in Tt.Ar, Ma.Ar, Ps.Pm, and Ec.Pm compared to euploid mice (Figure 3B-C,G-H). Male mice were increased in Tt.Ar, Ma.Ar, Ct.Ar, Ct.Th, Ps.Pm, and Ec.Pm compared to female mice at 6-weeks-old (Figure 3B-D,F-H). Sex-stratified one-tailed t-tests showed both male and female 6-week-old Ts66Yah mice having

significantly decreased Tt.Ar, Ma.Ar, Ps.Pm, and Ec.Pm compared to their respective euploid littermates, while only male Ts66Yah mice had significantly decreased Ct.Ar.

For cortical bone at 9 weeks of age, only Ma.Ar, Ct.Ar/Tt.Ar, and Ec.Pm had significant genotype effects (Figure 3C,E,H). Nine-week-old Ts66Yah mice had lower Ma.Ar and Ec.Pm but increased Ct.Ar/Tt.Ar compared to euploid mice. Sex effects were observed at 9-weeks-old in Tt.Ar, Ma.Ar, Ct.Ar, Ct.Th, Ps.Pm, Ec.Pm, and Ct.TMD, where male mice were greater than female mice (Figure 3B-D,F-I). Only male Ts66Yah mice had significantly decreased Tt.Ar, Ma.Ar, Ps.Pm, and Ec.Pm compared to their euploid littermates when sex-stratified one-tailed t-tests were performed, but both sexes had increased Ct.Ar/Tt.Ar while only male Ts66Yah mice had increased Ct.Th.

At 16 weeks of age, there were interactive effects of genotype and sex for Tt.Ar, Ma.Ar, Ps.Pm, and Ec.Pm. *Post hoc* analysis revealed male euploid mice had larger values than all other groups (male Ts66Yah, female euploid, and female Ts66Yah) for each parameter, and male Ts66Yah had larger values than both female groups in Tt.Ar and Ps.Pm. Sex effects were also present for Ct.Ar, Ct.Th, and Ct.TMD, where male mice had greater Ct.Ar and Ct.Th but smaller Ct.TMD compared to female mice. Sex-stratified one-tailed t-tests for Ct.Ar, Ct.Th, and Ct.TMD, indicated only Ct.Ar was significantly smaller in male Ts66Yah mice than male euploid mice. Female Ts66Yah mice had no significant differences in cortical parameters compared to female euploid mice at 16-weeks.

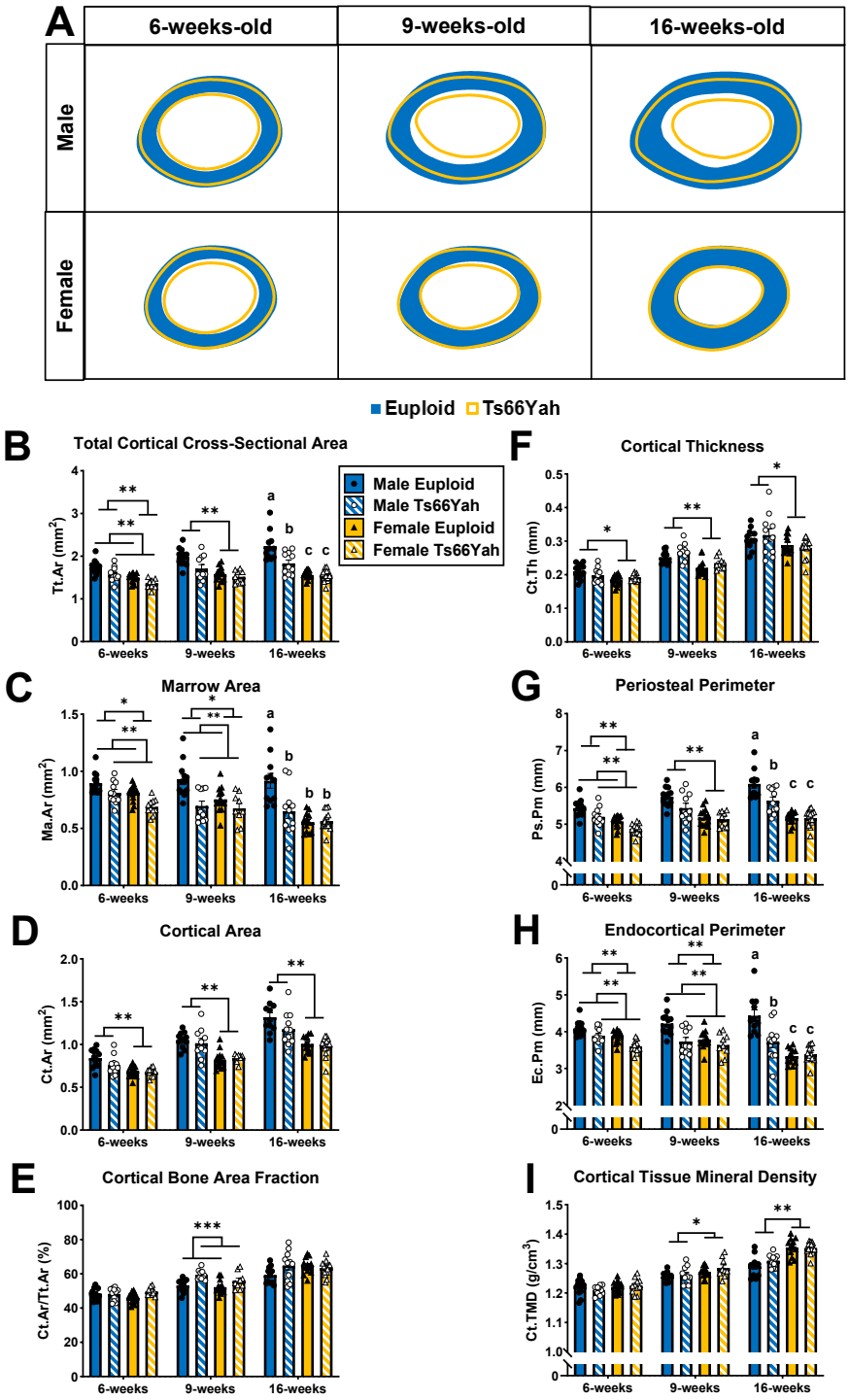

Figure 3: **Cortical bone analysis of 6-, 9-, and 16-week-old Ts66Yah mice. A)** Representations of the average cortical cross-section for each group made by calculating the centroid of each cortical section and finding the distance from the centroid to the endocortical and periosteal surfaces every 0.5 degrees. The average is found for each animal, then the average of the group is found to make the radar graph. **B-I)** Data are mean ± SEM. Different letters indicate $p < 0.05$ between groups as determined by Tukey or Games-Howell *post hoc* analysis of significant genotype × sex interaction. Asterisks indicate a sex or genotype effect as determined by two-way ANOVA. * $p < 0.05$, ** $p < 0.01$, *** $p < 0.001$. 6 weeks: male

euploid (n = 13), male Ts66Yah (n = 11), female euploid (n = 14), female Ts66Yah (n = 11); 9 weeks: male euploid (n = 12), male Ts66Yah (n = 10), female euploid (n = 13), female Ts66Yah (n = 9); 16 weeks: male euploid (n = 11), male Ts66Yah (n = 11), female euploid (n = 12), female Ts66Yah (n = 15).

Next, the mechanics and overall strength of the femurs was evaluated by the three-point bend test. For 6-week-old mice, genotype and sex effects were present for ultimate force, where euploid mice had a significantly greater ultimate force than Ts66Yah mice, and male mice had a greater ultimate force than female mice (Figure 4A; Table 1). At 9 weeks, genotype effects were found for postyield work and total work, where euploid mice were significantly greater than Ts66Yah mice, and sex effects were found for ultimate force, and stiffness, where male mice were significantly greater than female mice (Figure 4C; Table 1). At 16 weeks, a genotype effect was found for stiffness, where euploid mice were greater than Ts66Yah, and a sex effect was found for ultimate force, where male mice were greater than female mice (Figure 4E; Table 1). Additionally, an interaction was found for displacement. *Post hoc* analysis showed female euploid mice had the greatest total displacement compared to all other groups.

Six-week-old mice had a significant sex effect for yield stress, where female mice were greater than male mice (Figure 4B; Table 2). Genotype effects were found for yield stress and modulus at 9 weeks, showing Ts66Yah mice were greater than euploid mice (Figure 4D; Table 2). At 16 weeks, sex effects were detected for yield stress, modulus, resilience, and toughness, indicating female mice were significantly greater than male mice (Figure 4F; Table 2). Yield stress and toughness also showed interactions. For yield stress, male euploid mice were greater than both female euploid and Ts66Yah mice. For toughness, female euploid mice had the greatest toughness compared to all other groups.

Sex-stratified one-tailed t-tests showed both sexes of 6-week-old Ts66Yah mice had significantly decreased ultimate force compared to their euploid littermates, while only female Ts66Yah mice had significantly increased yield stress. At 9 weeks, male Ts66Yah mice had significantly increased yield stress and modulus and significantly decreased postyield work and

total work compared to male euploid littermates. At 16 weeks, male Ts66Yah mice had significantly decreased ultimate force and stiffness but significantly increased modulus compared to male euploid littermates. Sixteen-week-old female Ts66Yah mice were significantly decreased compared to female euploid littermates in resilience and toughness.

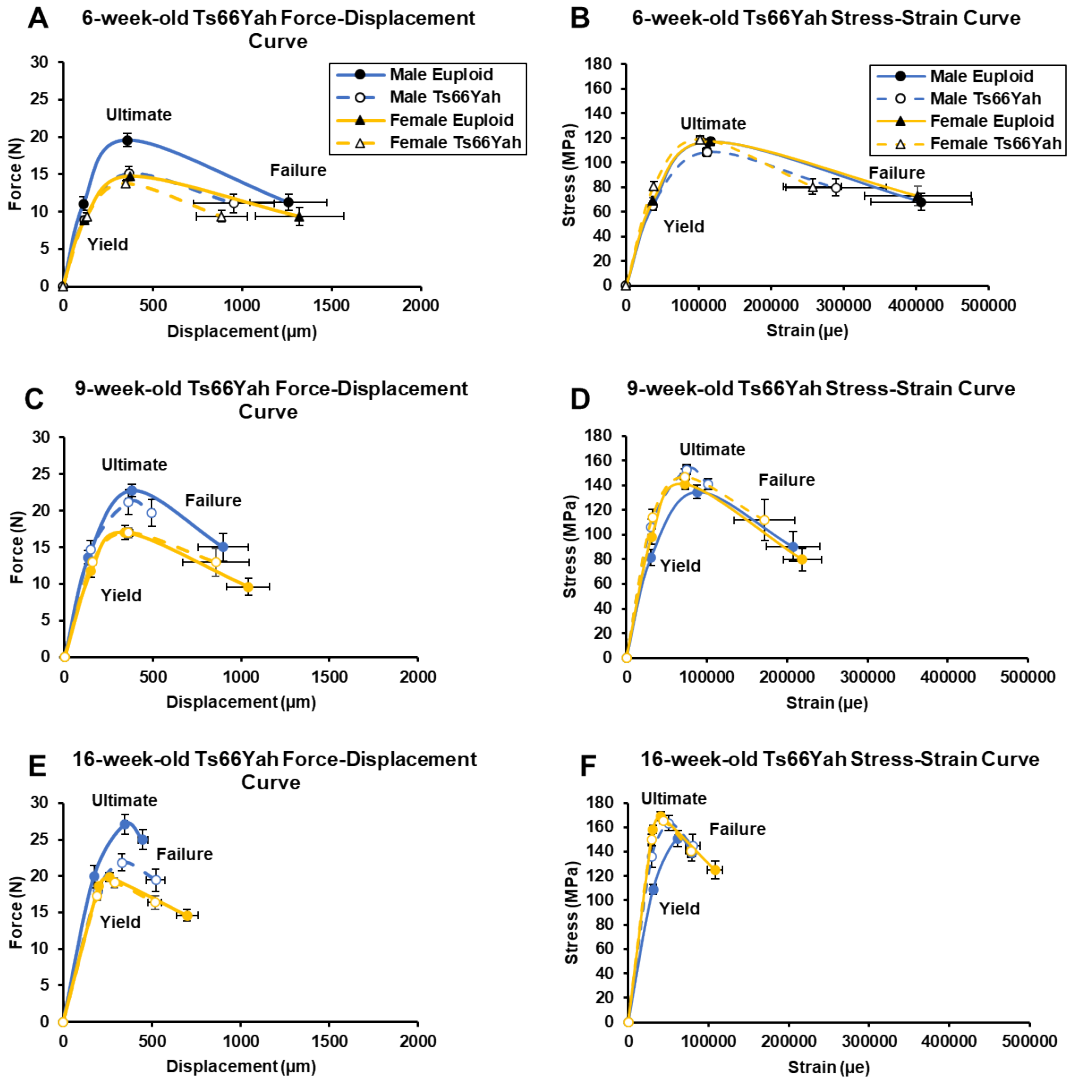

Figure 4: **Mechanical curves generated from 3-point femur bend of 6-, 9- and 16-week-old Ts66Yah mice.** Data are mean ± SEM. 6 weeks: male euploid (n = 12), male Ts66Yah (n = 11), female euploid (n = 11), female Ts66Yah (n = 11); 9 weeks: male euploid (n = 12), male Ts66Yah (n = 10), female euploid (n = 13), female Ts66Yah (n = 9); 16 weeks: male euploid (n = 11), male Ts66Yah (n = 11), female euploid (n = 12), female Ts66Yah (n = 15).

Table 1: **Whole bone (extrinsic) mechanical properties of 6-, 9-, and 16-week-old Ts66Yah mice.** Data are mean ± SEM. Different letters indicate $p < 0.05$ between groups as determined by Tukey or Games-Howell *post hoc* analysis of significant genotype × sex interaction. * indicates $p < 0.05$ as determined by sex-stratified one-tail t-test. 6 weeks: male euploid (n = 12), male Ts66Yah (n = 11), female euploid (n = 11), female Ts66Yah (n = 11); 9 weeks: male euploid (n = 12), male Ts66Yah (n = 10), female euploid (n = 13), female Ts66Yah (n = 9); 16 weeks: male euploid (n = 11), male Ts66Yah (n = 11), female euploid (n = 12), female Ts66Yah (n = 15).

	Yield Force	**Ultimate Force**	**Displacement to Yield**	**Postyield Displacement**	**Total Displacement**	**Stiffness**	**Work to Yield**	**Postyield Work**	**Total Work**
6-week-old									
Male Euploid	11.03 ± 0.904	19.58 ± 0.882	114.02 ± 5.42	1146 ± 213	1260 ± 214	101.73 ± 5.52	0.687 ± 0.084	15.37 ± 2.27	16.06 ± 2.32
Male Ts66Yah	8.93 ± 0.414	15.12 ± 1.000*	119.74 ± 5.10	833.18 ± 226.9	952.92 ± 225.4	80.59 ± 4.96	0.564 ± 0.037	9.85 ± 2.22	10.41 ± 2.22
Female Euploid	8.85 ± 0.385	14.79 ± 0.364	120.51 ± 6.37	1200 ± 246	1321 ± 249	79.87 ± 4.95	0.566 ± 0.039	10.80 ± 1.48	11.37 ± 1.49
Female Ts66Yah	9.40 ± 0.434	13.78 ± 0.404*	132.20 ± 3.52	753.64 ± 140.6	885.83 ± 140.9	75.60 ± 3.43	0.656 ± 0.038	8.22 ± 1.03	8.87 ± 1.03
9-week-old									
Male Euploid	13.63 ± 0.908	22.77 ± 0.885	133.95 ± 8.49	763.50 ± 147.0	897.45 ± 143.3	110.0 ± 4.50	1.01 ± 0.115	12.34 ± 1.88	13.34 ± 1.84
Male Ts66Yah	14.65 ± 1.267	21.20 ± 1.724	148.91 ± 4.95	346.50 ± 14.35	495.41 ± 14.87	104.72 ± 7.00	1.18 ± 0.129	6.58 ± 0.39	7.76 ± 0.50
Female Euploid	11.74 ± 0.829	17.03 ± 0.992	149.65 ± 7.53	892.23 ± 122.5	1042 ± 122	84.57 ± 4.14	0.959 ± 0.098	10.72 ± 0.88	11.68 ± 0.88
Female Ts66Yah	13.02 ± 0.424	16.97 ± 0.642	159.96 ± 6.42	695.89 ± 186.0	855.85 ± 187.1	87.94 ± 3.27	1.11 ± 0.069	8.22 ± 1.42*	9.33 ± 1.42*
16-week-old									
Male Euploid	19.93 ± 1.53	27.11 ± 1.34	173.11 ± 14.9	275.00 ± 34.63	448.11 ± 27.42[a]	126.46 ± 6.49	1.92 ± 0.311	6.81 ± 0.913	8.73 ± 0.848
Male Ts66Yah	17.84 ± 0.903	21.88 ± 1.20*	192.69 ± 7.76	328.27 ± 53.35	520.96 ± 54.20[a]	101.23 ± 6.55*	1.82 ± 0.121	6.49 ± 0.974	8.31 ± 0.967
Female Euploid	18.57 ± 0.556	19.84 ± 0.652	199.35 ± 3.40	498.17 ± 60.28	697.52 ± 60.86[b]	100.38 ± 3.87	2.00 ± 0.070	8.52 ± 0.882	10.51 ± 0.916
Female Ts66Yah	17.30 ± 0.630	19.06 ± 0.651	191.64 ± 5.99	325.73 ± 38.75	517.37 ± 37.96[a]	98.08 ± 3.59	1.80 ± 0.106	5.63 ± 0.603	7.43 ± 0.600

Table 2: **Material (intrinsic) mechanical properties of 6-, 9-, and 16-week-old Ts66Yah mice.** Data are mean ± SEM. Different letters indicate $p < 0.05$ between groups as determined by Tukey or Games-Howell *post hoc* analysis of significant genotype × sex interaction. * indicates $p < 0.05$ as determined by sex-stratified one-tail t-test. 6 weeks: male euploid (n = 12), male Ts66Yah (n = 11), female euploid (n = 11), female Ts66Yah (n = 11); 9 weeks: male euploid (n = 12), male Ts66Yah (n = 10), female euploid (n = 13), female Ts66Yah (n = 9); 16 weeks: male euploid (n = 11), male Ts66Yah (n = 11), female euploid (n = 12), female Ts66Yah (n = 15).

	Yield Stress	**Ultimate Stress**	**Strain to Yield**	**Total Strain**	**Modulus**	**Resilience**	**Toughness**
6-week-old							
Male Euploid	65.25 ± 3.60	117.28 ± 2.46	36860 ± 1749	406939 ± 69443	1.89 ± 0.083	1.30 ± 0.122	30.37 ± 3.94
Male Ts66Yah	64.84 ± 2.29	108.51 ± 3.59	36074 ± 1361	288994 ± 68900	1.92 ± 0.067	1.24 ± 0.077	22.73 ± 4.89
Female Euploid	69.62 ± 1.69	116.98 ± 2.22	37141 ± 11965	402180 ± 73850	2.04 ± 0.089	1.37 ± 0.088	28.28 ± 4.11
Female Ts66Yah	81.19 ± 3.61*	118.77 ± 2.55	38400 ± 953	256826 ± 39572	2.24 ± 0.083	1.65 ± 0.100	22.30 ± 2.64
9-week-old							
Male Euploid	81.55 ± 6.62	134.79 ± 5.38	30698 ± 1915	207424 ± 33870	2.86 ± 0.153	1.39 ± 0.175	17.75 ± 2.23
Male Ts66Yah	106.4 ± 5.96*	152.7 ± 3.95	30634 ± 1362	101401 ± 2369	3.77 ± 0.206*	1.74 ± 0.139	11.65 ± 0.500
Female Euploid	98.44 ± 6.41	141.1 ± 4.60	31593 ± 1549	218855 ± 23915	3.36 ± 0.176	1.69 ± 0.153	20.52 ± 1.35
Female Ts66Yah	113.9 ± 7.02	147.0 ± 6.67	31930 ± 1184	172033 ± 38007	3.86 ± 0.253	1.93 ± 0.132	16.38 ± 2.69
16-week-old							
Male Euploid	109.0 ± 3.81[a]	150.9 ± 6.48	317071 ± 3533	79006 ± 5153	4.09 ± 0.285	1.83 ± 0.234	8.49 ± 0.745[a]
Male Ts66Yah	135.8 ± 8.97[a,b]	163.4 ± 6.01	29306 ± 888.16	80175 ± 9012	4.99 ± 0.320*	2.12 ± 0.172	9.54 ± 1.13[a]
Female Euploid	158.2 ± 3.29[b]	168.8 ± 3.60	30840 ± 630.10	108200 ± 9548	5.53 ± 0.168	2.63 ± 0.077	13.70 ± 0.994[b]
Female Ts66Yah	150.2 ± 3.96[b]	165.0 ± 2.12	28678 ± 717.26	77739 ± 5657	5.67 ± 0.120	2.34 ± 0.109*	9.67 ± 0.734[a]

Germline reduction of Dyrk1a *copy number improves, but does not rescue, cortical deficits in male Ts66Yah mice at postnatal day 36*

To evaluate the role of trisomic *Dyrk1a* in the appendicular skeleton of Ts66Yah mice, Ts66Yah femurs with a germline reduction of *Dyrk1a* copy number were analyzed at P36. Male Ts66Yah mice had significantly shorter femurs than male euploid littermates (Supplemental Figure 2B). Male euploid,*Dyrk1a*$^{+/-}$ mice had the smallest body weight and femur length of all four male groups (Supplemental Figure 2). Female euploid,*Dyrk1a*$^{+/-}$ mice had the smallest body weight of all four female groups and a significantly shorter femur than female Ts66Yah and Ts66Yah,*Dyrk1a*$^{+/+/-}$ mice.

None of the trabecular bone parameters were significantly different in male or female Ts66Yah mice compared to their euploid littermates by sex-stratified, one-way ANOVA (Supplemental Figure 3). However, Tb.Th was significantly decreased in male Ts66Yah,*Dyrk1a*$^{+/+/-}$ mice compared to male euploid mice, suggesting a potential negative effect of *Dyrk1a* copy number reduction. Male euploid,*Dyrk1a*$^{+/-}$ mice had significant deficits in BMD, BV/TV, Tb.Th, and Tb.N compared to all other male mice, and significantly increased Tb.Sp compared to euploid and Ts66Yah,*Dyrk1a*$^{+/+/-}$ mice. No significant trabecular differences were found in female mice.

Male euploid mice were significantly greater than all other groups for Tt.Ar, Ma.Ar, Ct.Ar, Ps.Pm, Ec.Pm, maximum moment of inertia (I_{max}), and minimum moment of inertia (I_{min}), indicating there was not a rescue of cortical parameters (Figure 5). However, male Ts66Yah,*Dyrk1a*$^{+/+/-}$ mice were significantly greater than male Ts66Yah mice in all of the same parameters except Ct.Ar, which could indicate improvement in cortical deficits. Both sexes of euploid,*Dyrk1a*$^{+/-}$ mice had the lowest Ct.Ar/Tt.Ar and Ct.Th compared to all other groups of their sex. No other significant cortical differences were found in female mice.

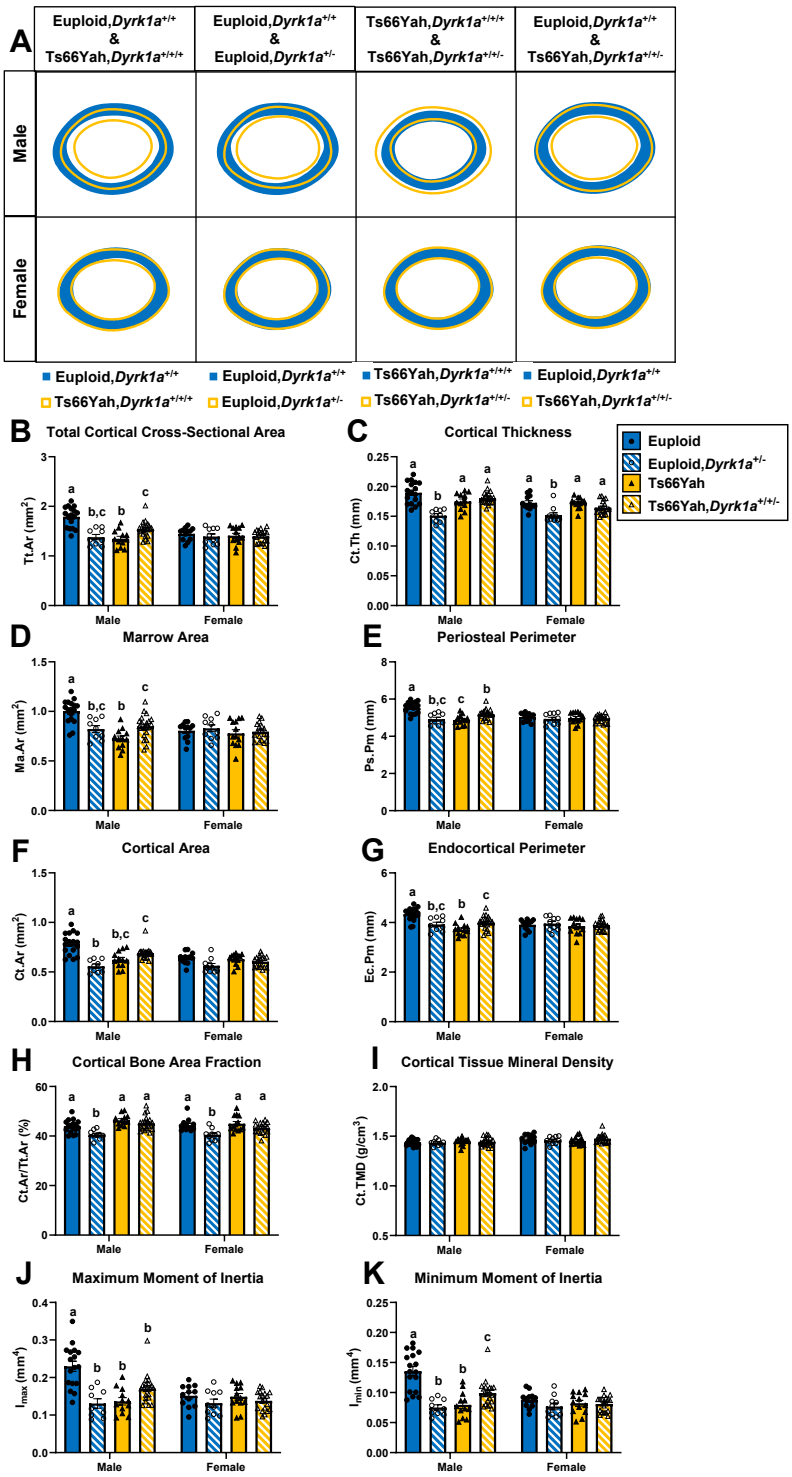

Figure 5: **Cortical bone parameters for P36 Ts66Yah,Dyrk1a$^{+/+/-}$ mice. A)** Representations of the average cortical cross-section for each group made by calculating the centroid of each cortical section and finding the distance from the centroid to the endocortical and periosteal surfaces every 0.5 degrees. The average is found for each animal, then the average of the group is found to make the radar graph. **B-K)** Data are mean ± SEM. Different letters indicate $p < 0.05$ between groups as determined by Tukey or Games-Howell *post hoc* analysis of significant sex-stratified one-way ANOVA. Male mice: euploid (n =

17); euploid,Dyrk1a$^{+/-}$ (n = 9); Ts66Yah (n = 12); Ts66Yah,Dyrk1a$^{+/+/-}$ (n = 21). Female mice: euploid (n = 12); euploid,Dyrk1a$^{+/-}$ (n = 10); Ts66Yah (n = 13); Ts66ah,Dyrk1a$^{+/+/-}$ (n = 19).

Treatment with Leucettinib-21, a DYRK1A inhibitor, did not improve skeletal deficits in Ts66Yah mice at postnatal day 36

To improve skeletal deficits in Ts66Yah mice, male and female mice were treated with 0.5mg/kg of Leucettinib-21 (L21) daily from postnatal day (P) 21 until P36 by oral gavage. As expected, both sexes of all groups increased body weight over the course of treatment (Figure 6A-B). There was a significant interaction between genotype and treatment in male mice only, driven by lower weight in Ts66Yah mice treated with L21 compared to the other three groups. Additionally, male mice had an interactive effect of postnatal day and treatment on body weight, where vehicle-treated mice began to weigh significantly more than L21-treated mice beginning on P27 and continuing through P36. This could indicate there are negative effects of L21 treatment during this time in male mice. Female mice had a significant overall genotype effect on body weight, but no significant differences on a particular postnatal day. These findings were confirmed by analyzing change in body weight over L21 treatment (calculated as weight at P21 subtracted from weight at P36); male mice had a significant treatment effect where vehicle-treated mice had a greater change in body weight than L21-treated mice, and female mice had a genotype effect where Ts66Yah mice had a greater change in body weight than euploid mice (Figure 6C).

For femur length, there was an interaction of genotype and treatment in male mice. *Post hoc* analysis showed male Ts66Yah mice treated with L21 had shorter femurs than euploid mice treated with L21 and Ts66Yah mice treated with the vehicle (Figure 6D). No significant differences were found in female mice. However, in both sexes, body weight at P36 is positively correlated with femur length at the same age, although the correlation is stronger in male mice

(Figure 6E-F). Together, these data indicate the low body weight of male Ts66Yah mice treated with L21 at the beginning of treatment may have influenced femoral length and structure independently of L21 treatment. .

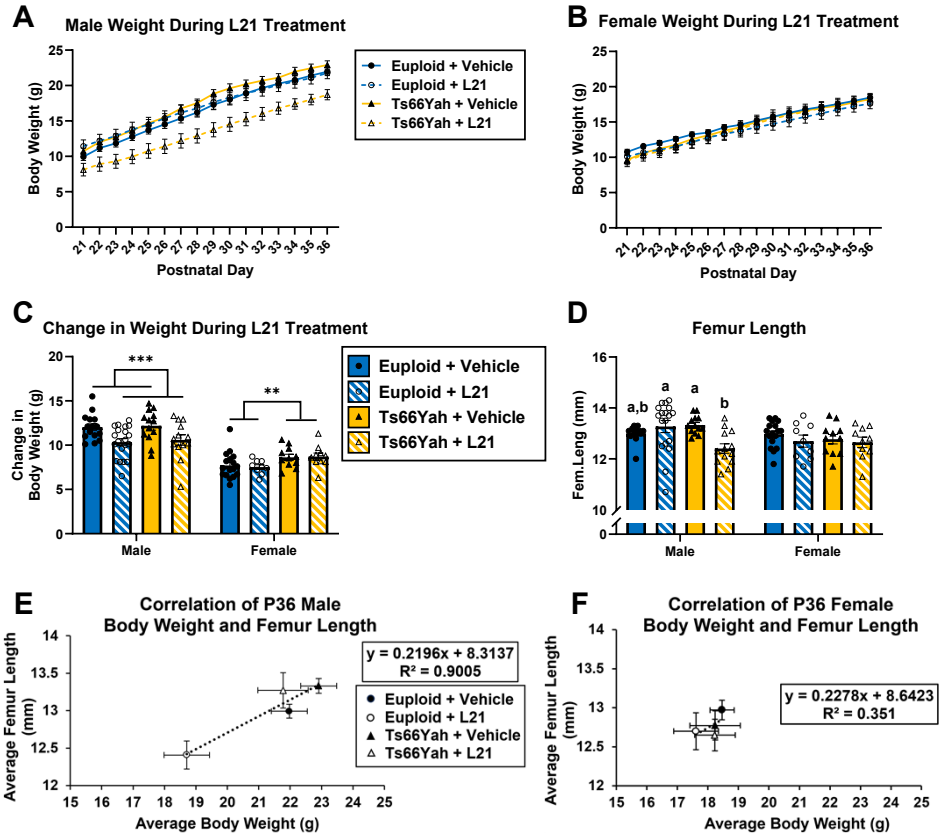

Figure 6 : **Body weight and femur lengths of Leucettinib-21-treated Ts66Yah mice.** Data are mean ± SEM. Different letters indicate $p < 0.05$ between groups as determined by Tukey or Games-Howell *post hoc* analysis of significant genotype × treatment interaction. Asterisks indicate a treatment or genotype effect as determined by sex-stratified two-way ANOVA. ** $p < 0.01$ and *** $p < 0.001$. Male mice: vehicle-treated euploid (n = 15 [weights] or 13 [femur length]), L21-treated euploid (n = 20 [weights] or 18 [femur length]), vehicle-treated Ts66Yah (n = 13), L21-treated Ts66Yah (n = 13). Female mice: vehicle-treated euploid (n = 17), L21-treated euploid (n = 9), vehicle-treated Ts66Yah (n = 11), L21-treated Ts66Yah (n = 10).

For trabecular parameters, significant genotype effects were found in male mice for BMD and BV/TV, which showed Ts66Yah mice having deficits compared to euploid mice (Supplemental Figure 4). For cortical parameters, interactive effects between genotype and treatment were detected in male mice for Tt.Ar, Ct.Ar, Ct.Th, Ps.Pm, I_{max}, and I_{min}. *Post hoc*

analysis for Ct.Th found a lower cortical thickness in L21-treated male Ts66Yah mice than vehicle-treated male Ts66Yah mice (Figure 7C). The remaining parameters found L21-treated male Ts66Yah mice as having the lowest value amongst all four groups (Figure 7). Significant treatment effects were also found for male mice in Ma.Ar and Ec.Pm, where vehicle-treated mice were greater than mice treated with L21. Significant genotype effects were found in all parameters of male mice except Ct.Th and Ct.TMD. For all but Ct.Ar/Tt.Ar, male Ts66Yah mice had deficits compared to male euploid mice. Female mice had no effects of treatment but had significant genotype effects for Tt.Ar, Ma.Ar, and Ec.Pm, all showing euploid mice as having a greater value than Ts66Yah mice.

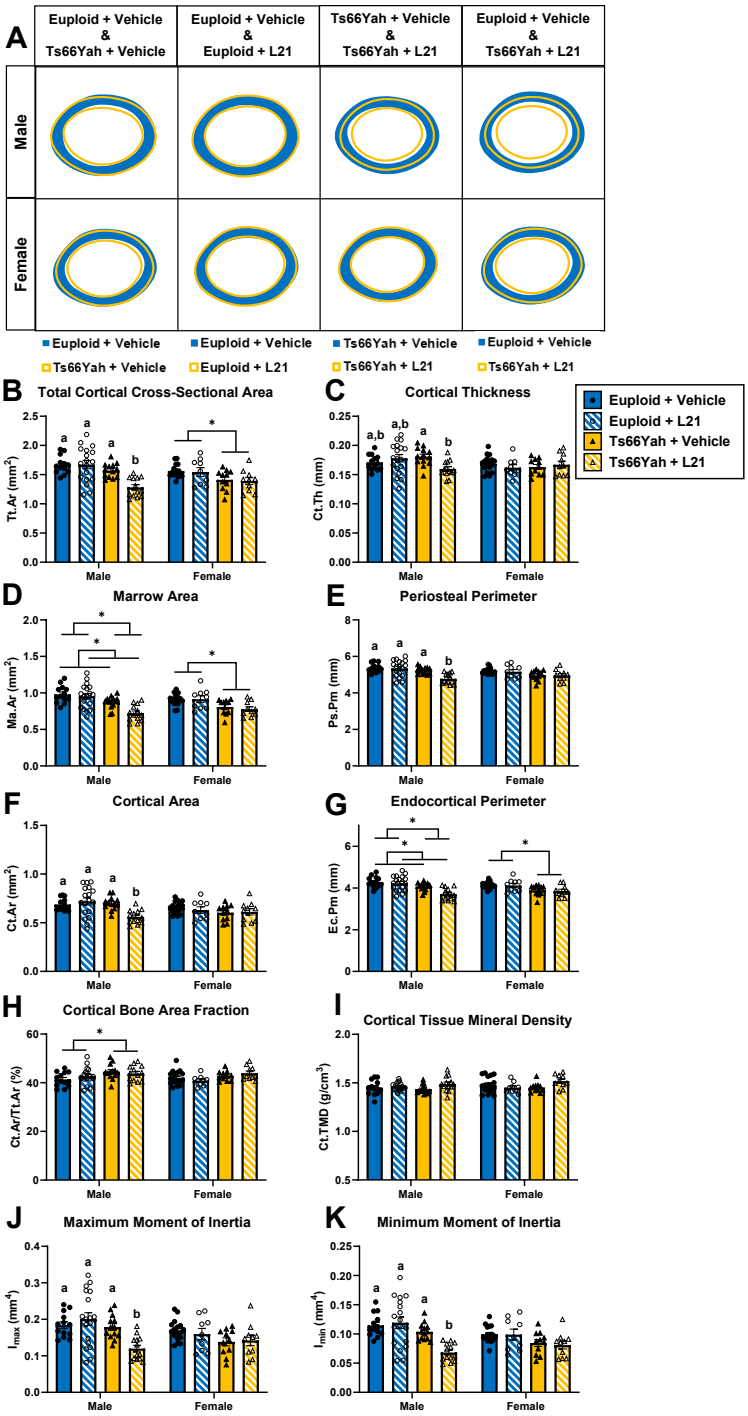

Figure 7: **Cortical bone parameters for Leucettinib-21-treated Ts66Yah mice. A)** Representations of the average cortical cross-section for each group made by calculating the centroid of each cortical section and finding the distance from the centroid to the endocortical and periosteal surfaces every 0.5 degrees. The average is found for each animal, then the average of the group is found to make the radar graph. **B-K)** Data are mean ± SEM. Different letters indicate $p < 0.05$ between groups as determined by Tukey or Games-Howell *post hoc* analysis of significant genotype × treatment interaction. Asterisks indicate a treatment or genotype effect as determined by two-way ANOVA. * $p < 0.05$. Male mice: vehicle-treated euploid (n = 13), L21-treated euploid (n = 18), vehicle-treated Ts66Yah (n = 13), L21-treated Ts66Yah (n

= 13). Female mice: vehicle-treated euploid (n = 17), L21-treated euploid (n = 9), vehicle-treated Ts66Yah (n = 11), L21-treated Ts66Yah (n = 10).

Ts65Dn and Ts66Yah mice are similar in their bone deficits at 6 and 16 weeks

6 weeks old: To find potential effects of the triplicated, non-Hsa21 homologous genes in the Ts65Dn as compared to the Ts66Yah mouse bone phenotypes, trabecular bone parameters were standardized for euploid Ts65Dn littermates, Ts65Dn mice, euploid Ts66Yah littermates, and Ts66Yah mice and then analyzed by principal component analysis (PCA) separately for male and female mice (Supplemental Figure 5A-B). Principal component 1 (PC1) was found to account for 92.68% of the variance for 6-week male trabecular bone parameters and 89.09% of the variance for female trabecular bone parameters (Supplemental Table 3). The coefficients (loadings) for each of the five parameters (BMD, BV/TV, Tb.Th, Tb.Sp, and Tb.N) for PC1 were nearly equal in magnitude for both sexes. However, Tb.Sp had a reverse sign compared to the other parameters. This is expected as Tb.Sp has been shown to be inversely correlated with the other trabecular parameters, and a higher trabecular separation is considered a skeletal deficit (SLOAN *et al.* 2023).

Since the first principal component (PC1) explains the most variance in the trabecular bone parameters, it was utilized to develop a single trabecular composite score. The composite score was assessed by 2-way ANOVA with mouse model and genotype, along with their interaction, as between-subject factors for each sex. The interaction term enables testing whether the difference in average trabecular composite score between euploid and trisomic mice differs between the two mouse models. The interaction was not significant for male (p = 0.944) or female (p = 0.093) mice. The mouse model main effect was also not significant for either sex (male p = 0.774, female p = 0.343), which is due to the standardization procedure. For male mice, there was a significant effect (p = 0.009) of genotype on trabecular composite

score; notably, for female mice, the genotype effect was not significant (p = 0.136). This indicates that Ts65Dn and Ts66Yah mice at 6 weeks have similar genotypic effects on trabecular bone, but only male mice exhibit significant deficits relative to respective euploid controls (Figure 8A-B).

PCA was performed separately for standardized cortical bone parameters (Tt.Ar, Ma.Ar, Ct.Ar, Ct.Th, Ps.Pm, Ec.Pm, and Ct.TMD) of 6-week-old male and female Ts65Dn and Ts66Yah mice (Supplemental Figure 5C-D). PC1 accounted for less percentage of the variance than for trabecular parameters at 67.3% and 61.94% for male and female mice, respectively (Supplemental Table 3). Two of the seven parameters, Ct.Th and Ct.TMD, contribute less to PC1 than the other five, which have roughly equal contributions. This is not surprising since Ct.TMD and Ct.Th are not always affected by trisomy depending on the mouse model and age (FOWLER *et al.* 2012; THOMAS *et al.* 2020; THOMAS *et al.* 2021; SHERMAN *et al.* 2022; LACOMBE *et al.* 2024; LAMANTIA *et al.* 2024).

As calculated with trabecular parameters, the PC1 loadings were utilized to develop the cortical composite score to be assessed by 2-way ANOVA. For male mice, there was a significant effect (p = 0.003) of genotype on cortical composite score. Female mice had a nearly significant genotype effect (p = 0.054). Neither sex exhibited a mouse model effect (male p = 0.384, female p = 0.505) nor interaction between genotype and mouse model (male p = 0.419, female p = 0.752). This indicates Ts65Dn and Ts66Yah mice have similar genotypic effects on cortical bone at 6 weeks, with deficits evident in both sexes, contrasting with trabecular deficits presenting only in males of both models (Figure 8C-D).

<u>16 weeks old:</u> The same method was performed using trabecular parameters (BV/TV, Tb.Th, Tb.Sp, and Tb.N) from 16-week-old male Ts65Dn and Ts66Yah mice (Supplemental Figure 5E). BMD was not included as Ts65Dn data was collected using dual-energy X-ray absorptiometry, resulting in an areal BMD, while Ts66Yah data was collected using µCT and

calibration of 0.25 & 0.75g/cm^3 hydroxyapatite phantoms, resulting in a volumetric BMD. PC1 accounted for 74.37% of the variance at this age (Supplemental Table 3). Tb.Th contributed less to the proportion of variance at 16 weeks than at 6 weeks, and Tb.Sp was still reversed in its sign. Two-way ANOVA of the male trabecular composite scores showed a significant genotype effect (p = 0.004) but no mouse model effect (p = 0.665) or interaction (p = 0.871). This indicates male Ts65Dn and Ts66Yah mice do not differ in the genotypic effects on trabecular phenotypes at 16 weeks and are at a deficit compared to euploid mice (Figure 8E). Female mice could not be compared due to a lack of data in female Ts65Dn mice at this age. Additionally, cortical measures could not be compared using this method due to a lack of comparable measures between Ts65Dn and Ts66Yah mice.

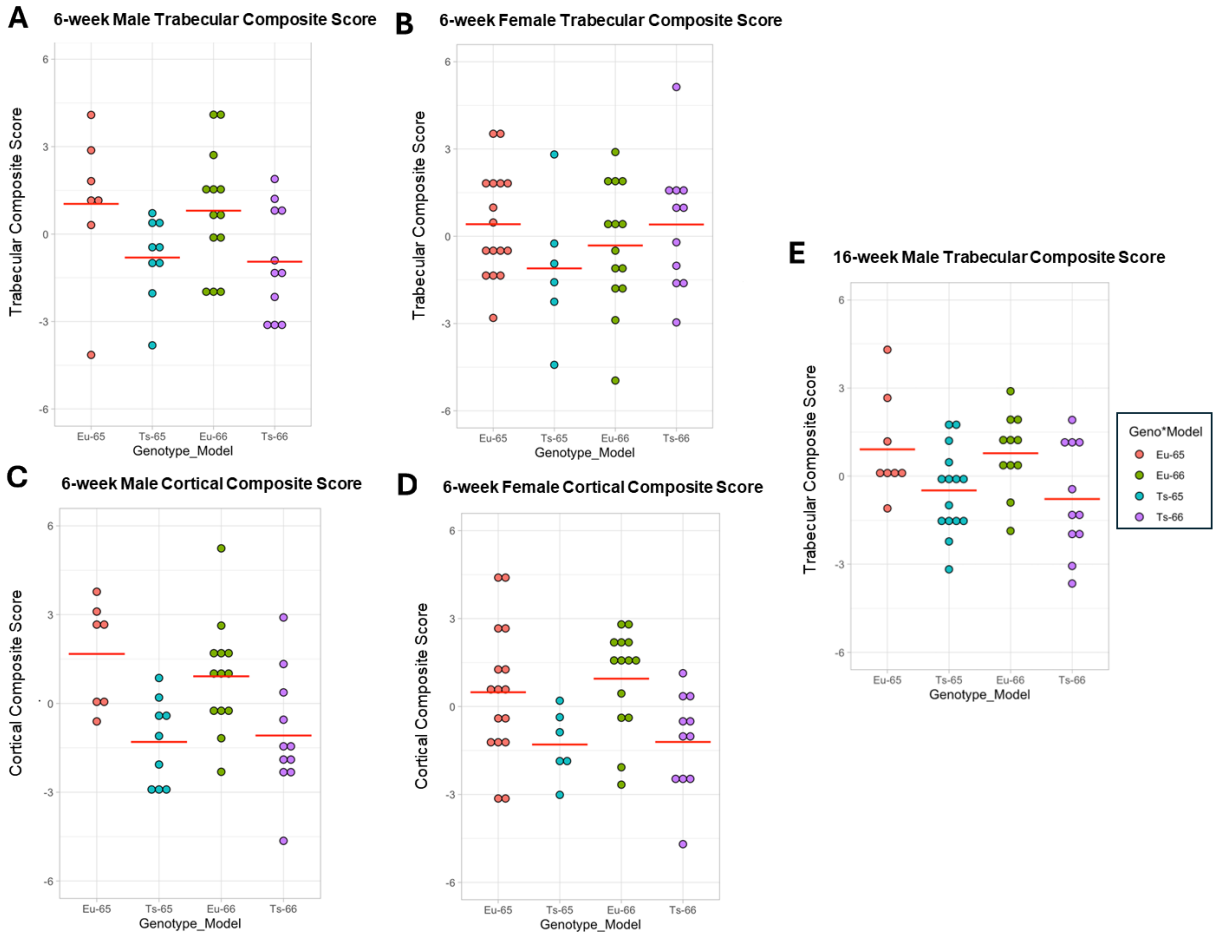

Figure 8: **Trabecular and cortical composite scores of 6- and 16-week-old Ts65Dn and Ts66Yah mice. A-B)** 6-week-old trabecular composite scores. **C-D)** 6-week-old cortical composite scores. **E)** 16-week-old male trabecular composite scores. Red horizontal line indicates group mean.

Differences between Ts65Dn and Ts66Yah skeletal phenotypes and effects of Dyrk1a *normalization are present at P36*

For P36 data, PCA was performed first on Ts65Dn and Ts66Yah mice and their respective euploid controls, as described for 6-week data (Supplemental Figure 6A-D). PC1 accounted for 85.6% and 85.5% of variance for male and female trabecular parameters, respectively (Supplemental Table 4). In both sexes, the loading of each trabecular parameter was similar in magnitude with Tb.Th contributing slightly less and Tb.Sp still reversed in sign. Two-way ANOVA of male trabecular composite scores showed a significant genotype effect ($p = 0.001$) and no mouse model effect ($p = 0.790$) or interaction ($p = 0.063$), where male euploid mice had higher trabecular composite scores than male trisomic mice (Figure 9A). Female trabecular composite scores showed a significant interaction between genotype and mouse model ($p = 0.037$), due to Ts65Dn mice showing a significantly lower score compared to euploid mice ($p = 0.042$) and Ts66Yah showing a non-significant, but higher score ($p = 0.400$) than their respective euploid control mice (Figure 9B).

For cortical parameters, PC1 accounted for 77.7% and 68.5% of variance for male and female mice, respectively (Supplemental Table 4). In male mice, the loading of most cortical parameters was similar in magnitude with Ct.Th contributing slightly less and Ct.TMD contributing very little and reversed in sign. In female mice, the loading was similar for all but Ct.Th and Ct.TMD; these were similar to each other except that Ct.TMD was reversed in sign. Two-way ANOVA of cortical composite scores found a significant genotype effect in male mice ($p < 0.001$) but not female mice ($p = 0.101$) and no significant effect of mouse model (male $p = 0.421$, female $p = 0.871$) or interaction (male $p = 0.989$, female $p = 0.313$) in either sex. This

indicates the Ts65Dn and Ts66Yah models do not differ in their genotypic effects on cortical phenotypes at P36 and male but not female mice show deficits compared to euploid mice (Figure 9C-D).

Next, PCA was performed on P36 Ts65Dn, Ts66Yah, and germline reduction of *Dyrk1a* copy number mice of each mouse model to understand if the effects of *Dyrk1a* copy number reduction from three copies to two varied between the two mouse models (Supplemental Figure 6E-H). For trabecular parameters, PC1 accounted for 80.6% and 85.1% of variance for male and female mice, respectively (Supplemental Table 4). In both sexes, the loading of all trabecular parameters except Tb.Th were similar in magnitude with Tb.Th contributing slightly less and Tb.Sp being reversed in sign. There was no main effect of mouse model or *Dyrk1a* copy number on trabecular composite score in either sex (male $p = 0.176$ and 0.0719, female $p = 0.153$ and 0.145) by two-way ANOVA. Notably, however, there was a significant interaction between mouse model and *Dyrk1a* copy number ($p = 0.0351$) in female mice, where Ts65Dn mice with 2 copies of *Dyrk1a* had a higher trabecular composite score whereas Ts66Yah mice with 2 copies of *Dyrk1a* had a lower trabecular composite score compared to their respective trisomic mice with 3 copies of *Dyrk1a* (Figure 9F). Male mice had a near significant interaction ($p = 0.058$) with a similar trend to female mice (Figure 9E). Together, this indicates that the effects of germline normalization of *Dyrk1a* copy number at P36 is dependent on mouse model and similar between sexes, where normalization is beneficial for Ts65Dn mice and negative for Ts66Yah mice.

For cortical parameters, PC1 accounted for 73.7% and 69.3% of the variance for male and female mice, respectively (Supplemental Table 4). In both sexes, the loadings of all cortical parameters except Ct.Th and Ct.TMD were similar in magnitude with Ct.Th contributing less and Ct.TMD contributing the least. However, Ct.Th seems to contribute more to male variance than female variance while the opposite is true for Ct.TMD. The sign of Ct.TMD was reversed in both

sexes. There were no significant main effects of mouse model (male $p = 0.600$, female $p = 0.507$) or *Dyrk1a* copy number (male $p = 0.407$, female $p = 0.408$), nor a significant interaction between them (male $p = 0.216$, female $p = 0.337$) on cortical composite score in either sex by two-way ANOVA, indicating *Dyrk1a* copy number does not rescue cortical deficits in either mouse model at P36 (Figure 9G-H).

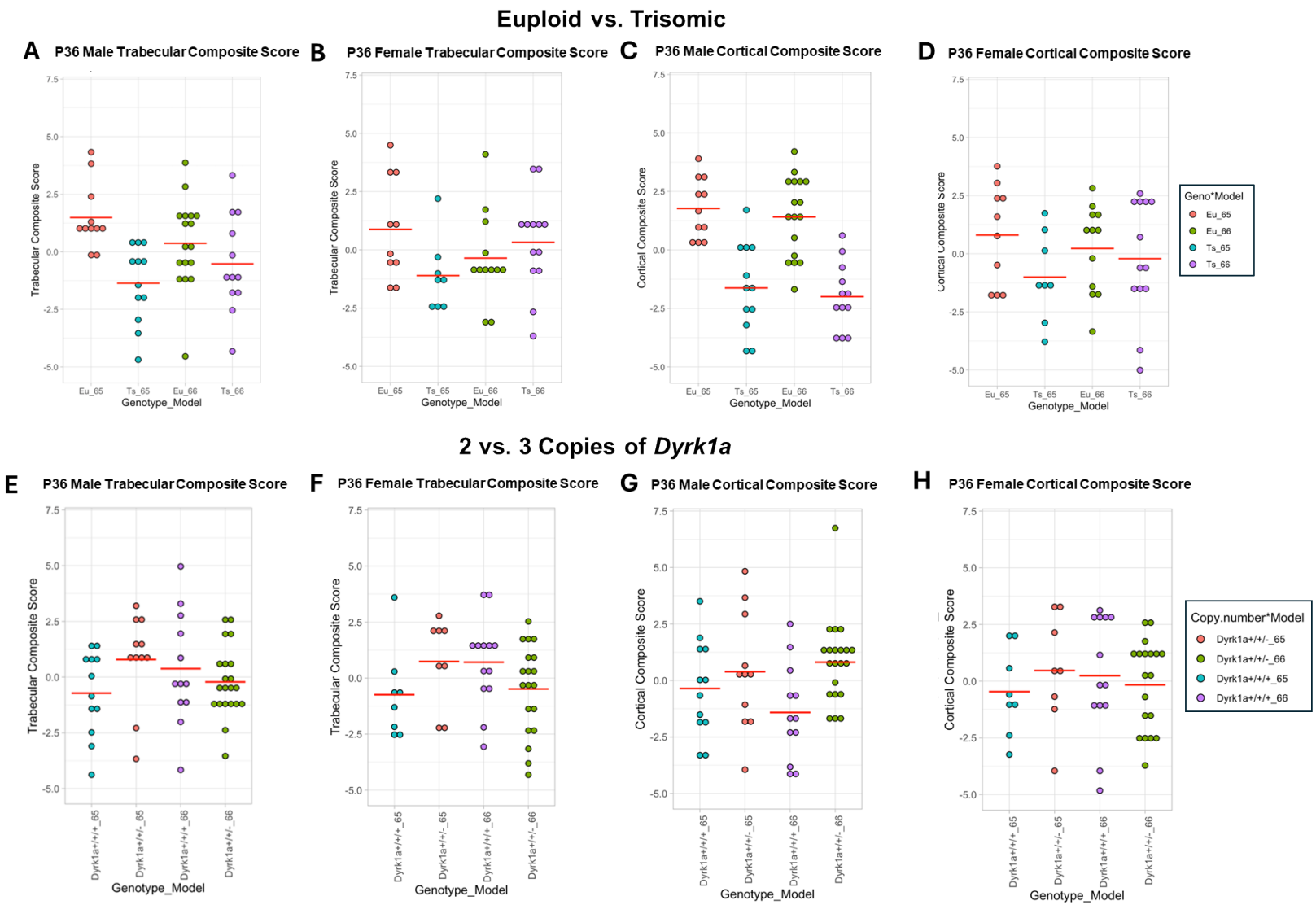

Figure 9: **Trabecular and cortical composite scores for P36 Ts65Dn, Ts66Yah, and germline reduction of *Dyrk1a* copy number mice. A-D)** Comparisons between euploid and trisomic mice. **E-H)** Comparisons between trisomic mice with 2 (*Dyrk1a*$^{+/+/-}$) or 3 (*Dyrk1a*$^{+/+/+}$) copies of *Dyrk1a*. Red horizontal line indicates group mean.

Discussion

Ts66Yah mice as a model for DS skeletal deficits

Previous research demonstrated that male Ts65Dn and Ts66Yah had similar cranial and mandibular deficits compared to euploid mice, but these deficits were less severe in male Ts66Yah mice compared to Ts65Dn mice (DUCHON *et al.* 2022). In the femur, trabecular bone of only male Ts66Yah mice displayed deficits at 6 and 16 weeks, which is consistent with findings in Dp1Tyb and Dp16Yey, two other mouse models of DS (Table 3) (THOMAS *et al.* 2020; LAMANTIA *et al.* 2024). Ts65Dn mice have previously shown trabecular deficits at 6 weeks in both sexes (THOMAS *et al.* 2021) and at 16 weeks in male mice (BLAZEK *et al.* 2011). The mature skeletal phenotype in female Ts65Dn mice is unknown, but female Dp1Tyb mice do not show trabecular deficits at 16 weeks (THOMAS *et al.* 2020), consistent with current findings in female Ts66Yah mice. Male Ts65Dn mice also show significant trabecular deficits at P36 (LACOMBE *et al.* 2024), which contrasts with current findings in male Ts66Yah mice. While Ts65Dn mice have not been investigated previously at 9 weeks of age, areal BMD was lower at the proximal tibia (including trabecular and cortical bone) in 8-week-old male Ts65Dn mice (WILLIAMS *et al.* 2018). This differs from what was found in Ts66Yah mice at 9 weeks of age, where skeletal phenotypes of the femur seem to normalize, perhaps due to differences in methodology and age. Bone growth is still occurring between 8 and 9 weeks in mice (JILKA 2013), and areal measurements of BMD can overestimate the severity of the deficit in DS due to a smaller bone size (CARFI *et al.* 2017; GARCIA-HOYOS *et al.* 2017). Additionally, the trabecular BMD reported in this paper and others from our lab does not include cortical bone whereas the BMD measurement of Williams *et al.* (2018) does. Since the tibial midshaft (cortical bone only) also has low BMD, it is possible the cortical bone included at the proximal tibia is driving the low BMD. Together, this may indicate the additional genes present in Ts65Dn mice result in trabecular deficits in (the case of female) or an earlier trabecular phenotype (in the case of

male). For example, high expression of *Fndc1* was implicated in contributing to trabecular bone loss in ovariectomized rats (XIAO *et al.* 2019).

Cortical phenotypes of male and female Ts66Yah mice appear to be consistent with Ts65Dn mice (Table 3). Male Ts65Dn mice exhibit cortical deficits at P36, 6 weeks, and 16 weeks while female mice exhibit deficits at 6 weeks (BLAZEK *et al.* 2011; THOMAS *et al.* 2021; LACOMBE *et al.* 2024). Again, it is unknown if female Ts65Dn mice have cortical deficits at 16 weeks, but female Dp1Tyb mice appear to have cortical deficits at 16 weeks (THOMAS *et al.* 2020). While the 16-week Dp1Tyb and Ts66Yah cortical phenotypes contrast, this may be the result of differing number of triplicated genes (~145 vs. ~100) and/or the transmission type of the triplicated gene content (segmental duplication vs. extra centromere). Additionally, female cortical bone phenotypes appear to vary with age in both Ts65Dn and Dp1Tyb/Dp16Yey mouse models: female Ts65Dn mice had deficits at P30 and P42 but not P36 (LACOMBE *et al.* 2024), female Dp1Tyb and Dp16Yey mice had deficits at 6 weeks (THOMAS *et al.* 2020; LAMANTIA *et al.* 2024), female Dp1Tyb mice had deficits at 16 weeks (THOMAS *et al.* 2020), yet female Dp16Yey mice did not have deficits at 12 weeks (SHERMAN *et al.* 2022). The lack of cortical deficits at 16 weeks in female Ts66Yah mice may been temporary and later ages may show the expected deficits.

Mechanics are often performed as a functional study of bone strength, as not all microarchitecture and geometry deficits or enhancements are sufficient to affect a bone's susceptibility to fracture. Alterations of whole bone mechanics, which can be affected by bone size, are found in Ts65Dn (BLAZEK *et al.* 2011; THOMAS *et al.* 2021), Dp1Tyb (THOMAS *et al.* 2020), Dp16Yey (LAMANTIA *et al.* 2024) and Ts66Yah mice (this study). The most common alteration is a decreased ultimate force, which is present in both sexes of all four models at 6-weeks-old and only male mice of the three models analyzed at 16-weeks-old. Material properties estimate the tissue level mechanics by normalizing whole bone mechanics using

bone size, so alterations in material properties may not be present even if whole bone mechanics are altered. Alterations in material properties were found in 6-week-old female Ts65Dn, Ts66Yah, and Dp16Yey mice but not Dp1Tyb mice, and 6-week-old male mice were only affected in the Dp16Yey model. Although material properties have not been evaluated in 16-week-old Ts65Dn or Dp16Yey animals, both male and female Ts66Yah and Dp1Tyb show alterations in material properties. Taken together, these data illustrate that alterations in mechanics are generally conserved between mouse models of DS.

Table 3: **Comparison of appendicular skeletal deficits in multiple mouse models of Down syndrome.** = indicates the model largely does not significantly differ from its euploid control, ↓ indicates the model is at a significant deficit compared to its euploid control, ↑ indicates the model is significantly improved compared to its euploid control, □ indicates there was a significant difference between the model and its euploid control, N/A indicates the data was unavailable, and ‡ indicates the data comes from a measurement including both trabecular and cortical bone. All Ts66Yah interpretations were made using data from this paper. P36 Ts65Dn interpretations were made using data from (LACOMBE *et al.* 2024). 6 week Ts65Dn interpretations were made using data from (THOMAS *et al.* 2021). 8 and 12 week Ts65Dn interpretations were made using data from (WILLIAMS *et al.* 2018). 16 week Ts65Dn interpretations were made using data from (BLAZEK *et al.* 2011). Dp1Tyb interpretations were made using data from (THOMAS *et al.* 2020). 6 week Dp16Yey interpretations were made using data from (LAMANTIA *et al.* 2024). 16 week Dp16Yey interpretations were made using data from (SHERMAN *et al.* 2022).

Male	**Ts66Yah**				**Ts65Dn**					**Dp1Tyb**		**Dp16Yey**	
	P36	*6 wks*	*9 wks*	*16 wks*	*P36*	*6 wks*	*8 wks*	*12 wks*	*16 wks*	*6 wks*	*16 wks*	*6 wks*	*12 wks*
Trabecular	=	↓	=	↓	↓	↓	↓‡	↓	↓	↓	↓	↓	↓
Cortical	↓	↓	↓/↑	↓	↓	↓	↓	↓	↓	↓	↓	↓	↓
Mechanics													
Whole Bone	N/A	□	□	□	N/A	□	N/A	N/A	□	□	□	□	N/A
Material	N/A	=	□	□	N/A	=	N/A	N/A	N/A	=	□	□	N/A

Female	**Ts66Yah**				**Ts65Dn**					**Dp1Tyb**		**Dp16Yey**	
	P36	*6 wks*	*9 wks*	*16 wks*	*P36*	*6 wks*	*8 wks*	*12 wks*	*16 wks*	*6 wks*	*16 wks*	*6 wks*	*12 wks*
Trabecular	=	=	=	=	=	=	N/A	N/A	N/A	=	=	=	=
Cortical	=	↓	=	=	=	↓	N/A	N/A	N/A	↓	↓	↓	=
Mechanics													
Whole Bone	N/A	□	=	=	N/A	□	N/A	N/A	N/A	□	□	□	N/A
Material	N/A	□	=	□	N/A	□	N/A	N/A	N/A	=	□	□	N/A

The effect of Dyrk1a *normalization differs between male Ts65Dn and Ts66Yah mice*

Reducing *Dyrk1a* copy number in Ts66Yah animals (Ts66Yah,*Dyrk1a*$^{+/+/-}$) did not affect trabecular bone at P36; however, there were also no significant deficits in male or female Ts66Yah mice with three copies of *Dyrk1a* compared to euploid animals at this age. The cortical bone size was significantly improved by *Dyrk1a* normalization at P36 but was not completely rescued in male Ts66Yah mice. This age was chosen for these experiments due to previous findings in male Ts65Dn animals, where normalization of *Dyrk1a* copy number by the same means as the current study resulted in improvement in all trabecular parameters and Ct.Th at P36 (LACOMBE *et al.* 2024). The lack of phenotypes in female mice with *Dyrk1a* copy number variation is consistent between the two models. It may be that non-Hsa21 orthologous, trisomic genes in male Ts65Dn mice work synergistically with *Dyrk1a* to result in earlier trabecular deficits that are amenable to *Dyrk1a* normalization but contribute more to cortical growth delay. For example, *Arid1b* is associated with growth delay by repressing canonical Wnt signaling (like DYRK1A) (VASILEIOU *et al.* 2015; LIU *et al.* 2020), and conditions related to *ARID1B* have noted delayed bone growth and age (VERGANO *et al.* 1993; TAN *et al.* 2022; TAO *et al.* 2022). *Dyrk1a* copy number normalization may improve trabecular deficits at a later age, as our previous study showed persistent trabecular deficits preceded *Dyrk1a*'s involvement (LACOMBE *et al.* 2024).

Pharmacological DYRK1A inhibition and confounding factors

Leucettinib-21 treatment may negatively affect male mouse growth as evidenced by L21-treated mice weighing significantly less than vehicle-treated mice from P27 until P36 and a significantly lower change in weight between the beginning and end of treatment. Despite these weight changes affecting both euploid and Ts66Yah mice, only L21-treated Ts66Yah mice appeared to have cortical bone and length deficits. These results may be confounded by an

initial weight difference between male Ts66Yah vehicle- and L21-treated mice at P21 (Figure 6A). Body weight differences often suggest lower bone mass, and body weight was found to correlate with femur length, so it is possible that the L21-treated male Ts66Yah group had a more severe bone phenotype than the vehicle-treated Ts66Yah group before treatment was administered. This makes it difficult to assess if the difference found in the femurs at P36 was due to Leucettinib-21 treatment or the innate differences between the groups. This may be due to the method of litter selection and treatment assignment or potential variability in the phenotype penetrance in Ts66Yah mice, which has been observed in individuals with DS.

There was also seemingly no difference in cortical bone between vehicle-treated male euploid and Ts66Yah mice, which contrasts with the results of the *Dyrk1a* reduction experiment at the same age. This could potentially be due to epigenetic factors or a result of the vehicle intubation treatment itself. The vehicle used in this study was 0.5% carboxymethylcellulose (CMC), which has been found to decrease osteoclastogenesis and increase osteoblastogenesis *in vitro* (AGIS *et al.* 2010; QI *et al.* 2018). It is possible treatment with CMC, either through known osteogenic properties or other epigenetic avenues, alleviates the cortical deficits in Ts66Yah mice. Nonetheless, the unexpected results of the vehicle-treated animals make it difficult to assess L21's potential as a treatment in this study.

Leucettinib cognitive treatment studies in DS mouse models are reviewed elsewhere (MEIJER *et al.* 2024). Two published studies have utilized Leucettinib-21 in mouse models of DS with no noted adverse effects despite the difference in age (embryos vs. adults) and tissue investigated (heart vs. brain) (LINDBERG *et al.* 2023; LANA-ELOLA *et al.* 2024). This illustrates the importance of timing the use of DYRK1A inhibitors for when *Dyrk1a* is overexpressed as implicated in previous studies (STRINGER *et al.* 2017b; LACOMBE *et al.* 2024). There also needs to be consideration the impact of DYRK1A inhibition on other non-target tissues. DYRK1A overexpression varies based on tissue and age (HAWLEY *et al.* 2023; LACOMBE *et al.* 2024),

which means treating cognitive deficits could worsen bone, as evidenced by previous EGCG treatments (JAMAL *et al.* 2022). This is not to say that DYRK1A inhibition treatments for tissue-specific deficits should stop, but that multiple tissues should be examined when treatments are tested to ensure the deterioration of one tissue is not at the expense of a slight improvement of another.

Periodic normalization of skeletal deficits in DS

At 9-weeks-old, male Ts66Yah mice had almost no trabecular deficits unlike at 6 and 16 weeks, illustrating a periodic developmental normalization of trabecular deficits. This has also been observed in male (P24 and P27) and female (P36) Ts65Dn mice in trabecular and cortical bone compartments (LACOMBE *et al.* 2024). It is suggested to occur in the Dp16Yey and Dp1Tyb mouse models as well, particularly for female Dp16Yey cortical phenotypes at 12 weeks (LAMANTIA *et al.* 2024). A similar phenomenon has also been noted in boys (11 to nearly 18 years old) and girls (10-16.5 years old) with DS in the cortical bone compartment, which was then termed a “bone recovery phase” that covered 2.5 years (GARN *et al.* 1972). Anthropometrical and radiological studies have also noted atypical non-linear growth and skeletal maturation rates in children and adolescents with DS, suggesting there is a period of time during childhood and adolescence (around 8-15 years of age) when children/adolescents with DS “catch-up” to and eventually surpass their chronological age (POZSONYI *et al.* 1964; RARICK *et al.* 1964; ROCHE 1967; RUNDLE *et al.* 1972).

Together, this illustrates that periodic normalization of skeletal deficits in multiple mouse models of DS are representative of individuals with DS. However, there is not yet a consensus on the timing of the periodic normalizations in each mouse model, which may be due to differences in the number of triplicated genes, which genes are triplicated, the transmission type

of triplicated genes, or lack of multiple timepoints with available data. More studies need to be conducted in both DS mouse models and individuals with DS to understand when and why these periodic normalizations occur. New therapies may be developed from understanding the mechanism behind these normalizations, and critical times for treatments can be better understood.

Direct comparisons of skeletal deficits in DS mouse models

Comparisons of bone parameter values between different mouse models of DS can be difficult due to conflated background strain effects (DEITZ AND ROPER 2011; PAPAGEORGIOU *et al.* 2020; FÖGER-SAMWALD *et al.* 2021) or methodological differences in measuring bone microstructure (e.g. using different µCT machines or different analyzers) (BONNET *et al.* 2009; VERDELIS *et al.* 2011). By standardizing each animal's value using the mean and standard deviation of all mice within each mouse model, these effects are minimized so direct comparisons can be made. Additionally, multiple parameters with varying degrees of correlation are obtained from each bone compartment of each animal and effects of trisomy may vary (SLOAN *et al.* 2023). This multivariate problem was addressed by using linear combinations of the standardized data to yield new (uncorrelated) variables via PCA. The first variable (principal component 1) explains the most variance in the standardized bone parameter values and is used to create a composite variable. Using this method, we have determined that skeletal phenotypes are not significantly different in male and female Ts65Dn and Ts66Yah femurs at 6 weeks, male femurs at 16 weeks, male trabecular bone at P36, or male and female cortical bone at P36. One notable exception was the presence of trabecular deficits in female Ts65Dn mice at P36 which were not present in female Ts66Yah mice, suggesting trisomic, non-Hsa21 orthologous genes in Ts65Dn may result in early, transient, sexually dimorphic trabecular deficits during bone accrual directly or through interactions with trisomic, Hsa21 orthologous

genes or disomic genes. Additionally, the effects of *Dyrk1a* copy number normalization at P36 did not differ significantly between Ts65Dn and Ts66Yah mice of either sex in cortical bone, but rescue of trabecular bone phenotypes with *Dyrk1a* normalization only occurred in Ts65Dn mice and may even worsen Ts66Yah trabecular bone.

This multivariate approach has also resulted in differing conclusions than interpreting parameters individually. Female Ts65Dn mice were suggested to have trabecular deficits at 6 weeks due to low BMD and high Tb.Sp (THOMAS *et al.* 2021), but these deficits were not sufficient to produce a significant deficit in trabecular composite score. The trabecular composite score findings suggest female Ts65Dn mice do not have a gross trabecular deficit at 6 weeks, which is consistent with trabecular phenotypes of other female DS mouse models (THOMAS *et al.* 2020; LAMANTIA *et al.* 2024). It was also suggested that *Dyrk1a* normalization at P36 improves male Ts66Yah (this study) and Ts65Dn cortical phenotypes (LACOMBE *et al.* 2024), but this did not produce a significantly increased cortical composite score in male trisomic mice with two functional copies of *Dyrk1a*. Additionally, female Ts65Dn mice had no deficits in any individual trabecular parameter (LACOMBE *et al.* 2024), but together, there is a significant decrease in trabecular composite score.

Statistically comparing DS mouse models across studies can be done in the future by utilizing the new described method with composite scores obtained from PCA. While it is currently used in the context of DS and single gene effects on skeletal phenotypes, the method may work with other DS phenotypic tests that pose a multivariate problem. Outside of the DS research community, this method can also be used for other μCT studies as an additional measure to objectively confirm gross deficits in trabecular and cortical regions, since it is uncommon for every parameter to be affected. Utilizing PCA to create a single composite variable will be most useful when the phenotypic variables are highly correlated and the first component is sufficient in explaining a large portion of the variation (SONG *et al.* 2013).

Otherwise, more than one component may be needed to capture the overall structure of the phenotypic data.

Conclusions

The trisomic, non-Hsa21 orthologous *Scaf8-Pde10a* region in Ts65Dn mice appears to modulate a small aspect of appendicular skeletal phenotypes by causing trabecular deficits in female mice. The benefit of *Dyrk1a* normalization is not present in the trabecular bone of Ts66Yah mice as in Ts65Dn mice but may appear at a later timepoint. Structural and mechanical evaluation of Ts66Yah mice indicate this is a potential model for DS-related appendicular skeletal phenotypes, but further evaluation of bone cellular dynamics and other skeletal sites should also be considered.

Competing Interests

The authors have no competing interests to declare.

Data Availability

Data has been uploaded to Dryad (DOI: 10.5061/dryad.kkwh70sf1). Reviewer URL: http://datadryad.org/stash/share/Wc0UyGfRfLvEzlF_FsYoCz7v4KjG9Gn2-y4F3hgutD8.

Funding

The research in this manuscript was supported by funds from the National Institutes of Health Eunice Kennedy Shriver National Institute for Child Health and Human Development

(https://www.nichd.nih.gov/) HD090603 (RJR) and the Jerome Lejeune Foundation (https://www.lejeunefoundation.org/) (RJR). The funders did not play any role in the study design, data collection and analysis, decision to publish, or preparation of the manuscript.

Acknowledgements

We thank Faith Prochaska, Isabella Crawford, Rebekah Hurd, and Joshua Lamantia for acquiring μCT scans, Dr. Laurent Meijer for providing the Leucettinib-21 and treatment protocol, and Claire Chevalier of Dr. Yann Herault's group for preparing Ts66Yah breeders for the IU Indianapolis colony. We also acknowledge the Small Animal Skeletal Phenotyping Core at the IU School of Medicine for the use of the SkyScan 1172.

CRediT Authorship Contribution Statement

Kourtney Sloan: Conceptualization, Methodology, Formal analysis, Investigation, Visualization, Supervision, Project administration, Writing – Original Draft

Kristina M. Piner: Formal analysis, Investigation, Writing – Review & Editing

Pathum Randunu Nawarathna Kandedura Arachchige: Conceptualization, Methodology, Formal analysis, Visualization, Writing – Review & Editing

Charles R. Goodlett: Conceptualization, Methodology, Supervision, Writing – Review & Editing

Yann Herault: Resources, Writing – Review & Editing

Gayla R. Olbricht: Conceptualization, Methodology, Supervision, Writing – Review & Editing

Joseph M. Wallace: Methodology, Software, Resources, Writing – Review & Editing

Randall J. Roper: Conceptualization, Resources, Funding acquisition, Supervision, Project administration, Writing – Original Draft

References

Adams, A. D., J. Lin, D. W. Bianchi, L. Bishop, T. Sato *et al.*, 2024 Embryonic statistical analyses reveal 2 growth phenotypes in mouse models of Down syndrome. Am J Obstet Gynecol 230**:** 258 e251-258 e211.

Agis, H., B. Beirer, G. Watzek and R. Gruber, 2010 Effects of carboxymethylcellulose and hydroxypropylmethylcellulose on the differentiation and activity of osteoclasts and osteoblasts. J Biomed Mater Res A 95**:** 504-509.

Alswat, K. A., 2017 Gender Disparities in Osteoporosis. J Clin Med Res 9**:** 382-387.

An, Q., D. Xu and G. P. Brooks, 2013 Type I Error Rates and Power of Multiple Hypothesis Testing Procedures in Factorial ANOVA. Multiple Linear Regression Viewpoints 39.

Antonarakis, S. E., B. G. Skotko, M. S. Rafii, A. Strydom, S. E. Pape *et al.*, 2020 Down syndrome. Nat Rev Dis Primers 6**:** 9.

Arron, J. R., M. M. Winslow, A. Polleri, C. P. Chang, H. Wu *et al.*, 2006 NFAT dysregulation by increased dosage of DSCR1 and DYRK1A on chromosome 21. Nature 441**:** 595-600.

Berman, A. G., C. A. Clauser, C. Wunderlin, M. A. Hammond and J. M. Wallace, 2015 Structural and Mechanical Improvements to Bone Are Strain Dependent with Axial Compression of the Tibia in Female C57BL/6 Mice. PLoS One 10**:** e0130504.

Blazek, J. D., I. Abeysekera, J. Li and R. J. Roper, 2015a Rescue of the abnormal skeletal phenotype in Ts65Dn Down syndrome mice using genetic and therapeutic modulation of trisomic Dyrk1a. Hum Mol Genet 24**:** 5687-5696.

Blazek, J. D., A. Gaddy, R. Meyer, R. J. Roper and J. Li, 2011 Disruption of bone development and homeostasis by trisomy in Ts65Dn Down syndrome mice. Bone 48**:** 275-280.

Blazek, J. D., A. M. Malik, M. Tischbein, M. L. Arbones, C. S. Moore *et al.*, 2015b Abnormal mineralization of the Ts65Dn Down syndrome mouse appendicular skeleton begins during embryonic development in a Dyrk1a-independent manner. Mech Dev 136**:** 133-142.

Bonnet, N., N. Laroche, L. Vico, E. Dolleans, D. Courteix *et al.*, 2009 Assessment of trabecular bone microarchitecture by two different x-ray microcomputed tomographs: a comparative study of the rat distal tibia using Skyscan and Scanco devices. Med Phys 36**:** 1286-1297.

Carfi, A., R. Liperoti, D. Fusco, S. Giovannini, V. Brandi *et al.*, 2017 Bone mineral density in adults with Down syndrome. Osteoporos Int 28**:** 2929-2934.

Costa, R., D. R. de Asua, A. Gullon, R. De Miguel, A. Bautista *et al.*, 2021 Volumetric BMD by 3D-DXA and Trabecular Bone Score in Adults With Down Syndrome. J Clin Densitom 24**:** 630-637.

Costa, R., A. Gullon, R. De Miguel, D. R. de Asua, A. Bautista *et al.*, 2018 Bone Mineral Density Distribution Curves in Spanish Adults With Down Syndrome. J Clin Densitom 21**:** 493-500.

de Graaf, G., F. Buckley, J. Dever and B. G. Skotko, 2017 Estimation of live birth and population prevalence of Down syndrome in nine U.S. states. Am J Med Genet A 173**:** 2710-2719.

Deitz, S. L., and R. J. Roper, 2011 Trisomic and allelic differences influence phenotypic variability during development of Down syndrome mice. Genetics 189**:** 1487-1495.

Duchon, A., M. Del Mar Muniz Moreno, C. Chevalier, V. Nalesso, P. Andre *et al.*, 2022 Ts66Yah, a mouse model of Down syndrome with improved construct and face validity. Dis Model Mech 15.

Duchon, A., M. Raveau, C. Chevalier, V. Nalesso, A. J. Sharp *et al.*, 2011 Identification of the translocation breakpoints in the Ts65Dn and Ts1Cje mouse lines: relevance for modeling Down syndrome. Mamm Genome 22**:** 674-684.

Egusa, H., M. Doi, M. Saeki, S. Fukuyasu, Y. Akashi *et al.*, 2011 The small molecule harmine regulates NFATc1 and Id2 expression in osteoclast progenitor cells. Bone 49**:** 264-274.

Föger-Samwald, U., M. Papageorgiou, K. Wahl-Figlash, K. Kerschan-Schindl and P. Pietschmann, 2021 Bone and muscle development in three inbred female mouse strains. Osteologie 30**:** 173-181.

Foley, C., and O. G. Killeen, 2019 Musculoskeletal anomalies in children with Down syndrome: an observational study. Arch Dis Child 104**:** 482-487.

Fotaki, V., M. Dierssen, S. Alcantara, S. Martinez, E. Marti *et al.*, 2002 Dyrk1A haploinsufficiency affects viability and causes developmental delay and abnormal brain morphology in mice. Mol Cell Biol 22**:** 6636-6647.

Fowler, T. W., K. D. McKelvey, N. S. Akel, J. Vander Schilden, A. W. Bacon *et al.*, 2012 Low bone turnover and low BMD in Down syndrome: effect of intermittent PTH treatment. PLoS One 7**:** e42967.

Garcia-Hoyos, M., M. T. Garcia-Unzueta, D. de Luis, C. Valero and J. A. Riancho, 2017 Diverging results of areal and volumetric bone mineral density in Down syndrome. Osteoporos Int 28**:** 965-972.

Garcia Hoyos, M., L. Humbert, Z. Salmon, J. A. Riancho and C. Valero, 2019 Analysis of volumetric BMD in people with Down syndrome using DXA-based 3D modeling. Arch Osteoporos 14**:** 98.

Garn, S. M., J. C. Gall, Jr. and J. M. Nagy, 1972 Preliminary radiogrammetric analysis of the bone recovery phase in adolescents with Down's syndrome. Invest Radiol 7**:** 97-101.

Goodlett, C. R., M. Stringer, J. LaCombe, R. Patel, J. M. Wallace *et al.*, 2020 Evaluation of the therapeutic potential of Epigallocatechin-3-gallate (EGCG) via oral gavage in young adult Down syndrome mice. Sci Rep 10**:** 10426.

Guedj, F., E. Kane, L. A. Bishop, J. L. A. Pennings, Y. Herault *et al.*, 2023 The Impact of Mmu17 Non-Hsa21 Orthologous Genes in the Ts65Dn Mouse Model of Down Syndrome: The Gold Standard Refuted. Biol Psychiatry 94**:** 84-97.

Hawley, L. E., M. Stringer, A. J. Deal, A. Folz, C. R. Goodlett *et al.*, 2023 Sex-specific developmental alterations in DYRK1A expression in the brain of a Down syndrome mouse model. Neurobiol Dis 190**:** 106359.

Henderson, A., S. A. Lynch, S. Wilkinson and M. Hunter, 2007 Adults with Down's syndrome: the prevalence of complications and health care in the community. Br J Gen Pract 57**:** 50-55.

Jamal, R., J. LaCombe, R. Patel, M. Blackwell, J. R. Thomas *et al.*, 2022 Increased dosage and treatment time of Epigallocatechin-3-gallate (EGCG) negatively affects skeletal parameters in normal mice and Down syndrome mouse models. PLoS One 17**:** e0264254.

Jilka, R. L., 2013 The relevance of mouse models for investigating age-related bone loss in humans. J Gerontol A Biol Sci Med Sci 68**:** 1209-1217.

Kim, H., K. S. Lee, A. K. Kim, M. Choi, K. Choi *et al.*, 2016 A chemical with proven clinical safety rescues Down-syndrome-related phenotypes in through DYRK1A inhibition. Dis Model Mech 9**:** 839-848.

Kohler, R., C. A. Tastad, A. J. Stacy, E. A. Swallow, C. E. Metzger *et al.*, 2021 The Effect of Single Versus Group muCT on the Detection of Trabecular and Cortical Disease Phenotypes in Mouse Bones. JBMR Plus 5**:** e10473.

Krieg, S., A. Krieg and K. Kostev, 2024 Age and sex-specific risk in fractures with Down syndrome in a retrospective case-control study from Germany. J Intellect Disabil Res.
LaCombe, J. M., K. Sloan, J. R. Thomas, M. P. Blackwell, I. Crawford *et al.*, 2024 Sex specific emergence of trisomic Dyrk1a-related skeletal phenotypes in the development of a Down syndrome mouse model. Dis Model Mech.
Lamantia, J., K. Sloan, J. M. Wallace and R. J. Roper, 2024 Compromised femoral and lumbovertebral bone in the Dp(16)1Yey Down syndrome mouse model. Bone 181**:** 117046.
Lana-Elola, E., R. Aoidi, M. Llorian, D. Gibbins, C. Buechsenschuetz *et al.*, 2024 Increased dosage of DYRK1A leads to congenital heart defects in a mouse model of Down syndrome. Sci Transl Med 16**:** eadd6883.
Lanzillotta, C., M. R. Baniowska, F. Prestia, C. Sette, V. Nalesso *et al.*, 2024 Shaping down syndrome brain cognitive and molecular changes due to aging using adult animals from the Ts66Yah murine model. Neurobiol Dis 196**:** 106523.
Lee, Y., J. Ha, H. J. Kim, Y. S. Kim, E. J. Chang *et al.*, 2009 Negative feedback Inhibition of NFATc1 by DYRK1A regulates bone homeostasis. J Biol Chem 284**:** 33343-33351.
Lindberg, M. F., E. Deau, F. Miege, M. Greverie, D. Roche *et al.*, 2023 Chemical, Biochemical, Cellular, and Physiological Characterization of Leucettinib-21, a Down Syndrome and Alzheimer's Disease Drug Candidate. J Med Chem 66**:** 15648-15670.
Liu, X., G. Hu, J. Ye, B. Ye, N. Shen *et al.*, 2020 De Novo ARID1B mutations cause growth delay associated with aberrant Wnt/beta-catenin signaling. Hum Mutat 41**:** 1012-1024.
Meijer, L., E. Chretien and D. Ravel, 2024 Leucettinib-21, a DYRK1A Kinase Inhibitor as Clinical Drug Candidate for Alzheimer's Disease and Down Syndrome. J Alzheimers Dis 101**:** S95-S113.
Moore, C. S., 2006 Postnatal lethality and cardiac anomalies in the Ts65Dn Down syndrome mouse model. Mamm Genome 17**:** 1005-1012.
Moyer, A. J., K. Gardiner and R. H. Reeves, 2021 All Creatures Great and Small: New Approaches for Understanding Down Syndrome Genetics. Trends Genet 37**:** 444-459.
Otte, E. D., and R. J. Roper, 2024 Skeletal health in DYRK1A syndrome. Front Neurosci 18**:** 1462893.
Papageorgiou, M., U. Foger-Samwald, K. Wahl, K. Kerschan-Schindl and P. Pietschmann, 2020 Age- and Strain-Related Differences in Bone Microstructure and Body Composition During Development in Inbred Male Mouse Strains. Calcif Tissue Int 106**:** 431-443.
Pozsonyi, J., D. Gibson and D. E. Zarfas, 1964 Skeletal Maturation in Mongolism (Down's Syndrome). J Pediatr 64**:** 75-78.
Qi, P., S. Ohba, Y. Hara, M. Fuke, T. Ogawa *et al.*, 2018 Fabrication of calcium phosphate-loaded carboxymethyl cellulose non-woven sheets for bone regeneration. Carbohydr Polym 189**:** 322-330.
Rarick, L., I. Rapaport and V. Seefeldt, 1964 Bone Development in Down's Disease; Osseous Development of the Bones of the Hand and Wrist in Mongolism (Down's Disease) during the Prepubescent and Pubescent Years. Am J Dis Child 107**:** 7-13.
Reinholdt, L. G., Y. Ding, G. J. Gilbert, A. Czechanski, J. P. Solzak *et al.*, 2011 Molecular characterization of the translocation breakpoints in the Down syndrome mouse model Ts65Dn. Mamm Genome 22**:** 685-691.
Roche, A. F., 1967 Skeletal maturation and elongation in Down's disease (mongolism). Eugen Rev 59**:** 11-21.
Roper, R. J., H. K. St John, J. Philip, A. Lawler and R. H. Reeves, 2006 Perinatal loss of Ts65Dn Down syndrome mice. Genetics 172**:** 437-443.
Rundle, A. T., E. Donoghue, K. A. Abbas and A. Krstic, 1972 A catch-up phenomenon in skeletal development of children with Down's syndrome. J Ment Defic Res 16**:** 41-47.

Seeman, E., 2003 Periosteal bone formation--a neglected determinant of bone strength. N Engl J Med 349**:** 320-323.
Sherman, K. M., D. K. Williams, C. A. Welsh, A. M. Cooper, A. Falck *et al.*, 2022 Low bone mass and impaired fracture healing in mouse models of Trisomy21 (Down syndrome). Bone 162**:** 116471.
Sloan, K., J. Thomas, M. Blackwell, D. Voisard, E. Lana-Elola *et al.*, 2023 Genetic dissection of triplicated chromosome 21 orthologs yields varying skeletal traits in Down syndrome model mice. Dis Model Mech 16.
Song, M. K., F. C. Lin, S. E. Ward and J. P. Fine, 2013 Composite variables: when and how. Nurs Res 62**:** 45-49.
Stringer, M., I. Abeysekera, J. Thomas, J. LaCombe, K. Stancombe *et al.*, 2017a Epigallocatechin-3-gallate (EGCG) consumption in the Ts65Dn model of Down syndrome fails to improve behavioral deficits and is detrimental to skeletal phenotypes. Physiol Behav 177**:** 230-241.
Stringer, M., C. R. Goodlett and R. J. Roper, 2017b Targeting trisomic treatments: optimizing Dyrk1a inhibition to improve Down syndrome deficits. Mol Genet Genomic Med 5**:** 451-465.
Sturgeon, X., and K. J. Gardiner, 2011 Transcript catalogs of human chromosome 21 and orthologous chimpanzee and mouse regions. Mamm Genome 22**:** 261-271.
Tan, Y., J. Chen, Y. Li, Y. Liu, Y. Wang *et al.*, 2022 Three Novel ARID1B Variations in Coffin-Siris Syndrome Patients. Neurol India 70**:** 2174-2179.
Tang, J. Y. M., H. Luo, G. H. Y. Wong, M. M. Y. Lau, G. M. Joe *et al.*, 2019 Bone mineral density from early to middle adulthood in persons with Down syndrome. J Intellect Disabil Res 63**:** 936-946.
Tao, D. Y., H. H. Niu, J. J. Zhang, H. Q. Zhang, M. H. Zeng *et al.*, 2022 Short stature and melanocytic nevi in a girl with ARID1B-related Coffin-Siris syndrome: a case report. BMC Pediatr 22**:** 486.
Thomas, J. R., J. LaCombe, R. Long, E. Lana-Elola, S. Watson-Scales *et al.*, 2020 Interaction of sexual dimorphism and gene dosage imbalance in skeletal deficits associated with Down syndrome. Bone**:** 115367.
Thomas, J. R., and R. J. Roper, 2021 Current Analysis of Skeletal Phenotypes in Down Syndrome. Curr Osteoporos Rep.
Thomas, J. R., K. Sloan, K. Cave, J. M. Wallace and R. J. Roper, 2021 Skeletal Deficits in Male and Female down Syndrome Model Mice Arise Independent of Normalized Dyrk1a Expression in Osteoblasts. Genes (Basel) 12.
van Allen, M. I., J. Fung and S. B. Jurenka, 1999 Health care concerns and guidelines for adults with Down syndrome. Am J Med Genet 89**:** 100-110.
Vasileiou, G., A. B. Ekici, S. Uebe, C. Zweier, J. Hoyer *et al.*, 2015 Chromatin-Remodeling-Factor ARID1B Represses Wnt/beta-Catenin Signaling. Am J Hum Genet 97**:** 445-456.
Verdelis, K., L. Lukashova, E. Atti, P. Mayer-Kuckuk, M. G. Peterson *et al.*, 2011 MicroCT morphometry analysis of mouse cancellous bone: intra- and inter-system reproducibility. Bone 49**:** 580-587.
Vergano, S. A., P. J. van der Sluijs and G. Santen, 1993 ARID1B-Related Disorder in *GeneReviews((R))*, edited by M. P. Adam, J. Feldman, G. M. Mirzaa, R. A. Pagon, S. E. Wallace *et al.*, Seattle (WA).
Williams, D. K., S. G. Parham, E. Schryver, N. S. Akel, R. S. Shelton *et al.*, 2018 Sclerostin Antibody Treatment Stimulates Bone Formation to Normalize Bone Mass in Male Down Syndrome Mice. JBMR Plus 2**:** 47-54.
Xiao, Y., R. Wei, Z. Yuan, X. Lan, J. Kuang *et al.*, 2019 Rutin suppresses FNDC1 expression in bone marrow mesenchymal stem cells to inhibit postmenopausal osteoporosis. Am J Transl Res 11**:** 6680-6690.

Xing, Z., Y. Li, E. Cortes-Gomez, X. Jiang, S. Gao *et al.*, 2023 Dissection of a down syndrome-associated trisomy to separate the gene dosage-dependent and -independent effects of an extra chromosome. Hum Mol Genet**:** 2205-2218.

Supplemental Tables and Figures

Supplemental Table 1: **Transmission of trisomy in Ts66Yah x B6C3F1 breeding scheme**. (*) to represent that animals that did not survive to weaning were included. ǂ indicates $p < 0.05$ based on chi-square goodness of fit test performed on total data.

	Ts66Yah x B6C3F1				
	Total	**2021**	**2022**	**2023**	**2024**
# of litters	114	22	52	28	11
Total animals*	559	113	255	129	62
Total trisomic*	248	49	118	52	29
% trisomic*	44.36%ǂ	43.36%	46.27%	40.31%	46.77%
Animals not surviving to weaning	19	1	8	8	2
Total trisomic	8	1	2	3	2
% trisomic	42.11%	100.00%	25.00%	37.50%	100.00%
Total weaned	540	112	247	121	60
Total males	283	58	128	70	27
Total trisomic males	124	26	57	30	11
% trisomic males	43.82%	44.83%	44.53%	42.86%	40.74%
Total females	257	54	119	51	33
Total trisomic females	116	22	59	19	16
% trisomic females	45.14%	40.74%	49.58%	37.25%	48.48%

Supplemental Table 2: **Transmission of trisomy in Ts66Yah x *Dyrk1a*$^{+/-}$ breeding scheme**. (*) to represent that animals that did not survive to weaning were included. ǂ indicates $p < 0.05$ based on chi-square goodness of fit test performed on total data.

				Ts66Yah x *Dyrk1a*$^{+/-}$			
	Total	**2022**	**2023**		**Total**	**2022**	**2023**
# of litters	26	11	15	**Total euploid wildtype***	32	12	20
				% euploid wildtype*	24.81%ǂ	18.75%	30.77%
Total animals*	129	64	65	**Total euploid mutant***	23	14	9
Total trisomic*	74	38	36	**% euploid mutant***	17.83%ǂ	21.88%	13.85%
% trisomic*	57.36%	59.38%	55.38%	**Total trisomic wildtype***	26	15	11
Total mutant *Dyrk1a**	71	37	34	**% trisomic wildtype***	20.16%ǂ	23.44%	16.92%
% mutant *Dyrk1a**	55.04%	57.81%	52.31%	**Total trisomic mutant***	48	23	25
				% trisomic mutant*	37.21%ǂ	35.94%	38.46%
Animals not surviving to weaning	3	1	2				
Total trisomic	1	0	1	**Total male euploid wildtype**	20	9	11
% trisomic	33.33%	0.00%	50.00%	**% male euploid wildtype**	15.87%ǂ	14.29%	17.46%
Total mutant *Dyrk1a*	3	1	2	**Total male euploid mutant**	10	8	2
% mutant *Dyrk1a*	100.00%	100.00%	100.00%	**% male euploid mutant**	7.94%ǂ	12.70%	3.17%
				Total male trisomic wildtype	14	8	6
Total weaned	126	63	63	**% male trisomic wildtype**	11.11%ǂ	12.70%	9.52%
Total males	69	35	34	**Total male trisomic mutant**	25	10	15
Total trisomic males	39	18	21	**% male trisomic mutant**	19.84%ǂ	15.87%	23.81%
% trisomic males	30.95%	28.57%	33.33%	**Total female euploid wildtype**	12	3	9
Total mutant males	35	18	17	**% female euploid wildtype**	9.52%ǂ	4.76%	14.29%
% mutant males	27.78%	28.57%	26.98%	**Total female euploid mutant**	11	5	6
Total females	57	28	29	**% female euploid mutant**	8.73%ǂ	7.94%	9.52%
Total trisomic females	34	20	14	**Total female trisomic wildtype**	12	7	5
% trisomic females	26.98%	31.75%	22.22%	**% female trisomic wildtype**	9.52%ǂ	11.11%	7.94%
Total mutant females	33	18	15	**Total female trisomic mutant**	22	13	9
% mutant females	26.19%	28.57%	23.81%	**% female trisomic mutant**	17.46%ǂ	20.63%	14.29%

Supplemental Table 3: **Results of principal components analysis (PCA) for trabecular (top panel) and cortical (bottom panel) parameters of 6- and 16-week-oldTs65Dn and Ts66Yah mice.** Six-week male and female Ts65Dn data from euploid littermates and Ts65Dn mice lacking OSX-cre (THOMAS *et al.* 2021). Sixteen-week male Ts65Dn data from (BLAZEK *et al.* 2011). N/A indicates data was not comparable, so it was not included in PCA. See Supplemental Figure 5 for PCA biplots.

	6-week Male	**6-week Female**	**16-week Male**	
	PC1	**PC1**	**PC1**	**PC2**
BMD	0.458	0.443	N/A	N/A
BV/TV	0.463	0.472	0.574	0.059
Tb.Th	0.423	0.423	0.244	0.937
Tb.Sp	-0.452	-0.435	-0.554	0.184
Tb.N	0.439	0.461	0.551	-0.291
Proportion of Variance	0.92684	0.89093	0.74369	0.23430

	6-week Male			**6-week Female**		
	PC1	**PC2**	**PC3**	**PC1**	**PC2**	**PC3**
Tt.Ar	0.459	0.053	0.031	0.479	0.001	0.051
Ma.Ar	0.389	0.413	0.231	0.427	0.319	0.164
Ct.Ar	0.416	-0.332	-0.191	0.372	-0.461	-0.15
Ct.Th	0.283	-0.608	-0.354	0.166	-0.677	-0.279
Ps.Pm	0.456	0.035	-0.086	0.478	0.005	-0.013
Ec.Pm	0.418	0.324	0.164	0.437	0.29	0.135
Ct.TMD	0.054	-0.491	0.866	-0.049	-0.378	0.923
Proportion of Variance	0.67295	0.19558	0.12497	0.61936	0.25222	0.12353

Supplemental Table 4: **Results of principal components analysis (PCA) for trabecular (top panel) and cortical (bottom panels) parameters of P36 Ts65Dn, Ts66Yah, and germline reduction of *Dyrk1a* copy number mice.** P36 male and female Ts65Dn data from (LACOMBE et al. 2024). See Supplemental Figure 6 for PCA biplots.

	P36 Male	P36 Female	P36 *Dyrk1a* Male	P36 *Dyrk1a* Female
	PC1	**PC1**	**PC1**	**PC1**
BMD	0.465	0.472	0.463	0.476
BV/TV	0.481	0.480	0.495	0.482
Tb.Th	0.397	0.364	0.377	0.351
Tb.Sp	-0.439	-0.445	-0.441	-0.443
Tb.N	0.450	0.465	0.452	0.472
Proportion of Variance	0.85611	0.85460	0.80567	0.85060

	P36 Male		P36 Female		
	PC1	**PC2**	**PC1**	**PC2**	**PC3**
Tt.Ar	0.427	0.036	0.455	0.021	0.091
Ma.Ar	0.410	0.151	0.433	0.203	0.227
Ct.Ar	0.417	-0.126	0.406	-0.352	-0.184
Ct.Th	0.351	-0.341	0.171	-0.703	-0.429
Ps.Pm	0.427	0.033	0.454	0.032	0.059
Ec.Pm	0.412	0.139	0.436	0.195	0.189
Ct.TMD	-0.026	-0.907	-0.121	-0.548	0.827
Proportion of Variance	0.77700	0.15983	0.68540	0.20966	0.10211

	P36 *Dyrk1a* Male			P36 *Dyrk1a* Female		
	PC1	**PC2**	**PC3**	**PC1**	**PC2**	**PC3**
Tt.Ar	0.438	0.025	0.105	0.451	0.036	0.100
Ma.Ar	0.414	0.166	0.334	0.422	0.283	0.188
Ct.Ar	0.419	-0.182	-0.271	0.397	-0.416	-0.077
Ct.Th	0.303	-0.427	-0.668	0.202	-0.764	-0.197
Ps.Pm	0.437	0.024	0.093	0.451	0.038	0.097
Ec.Pm	0.418	0.16	0.288	0.427	0.255	0.178
Ct.TMD	-0.056	-0.855	0.516	-0.186	-0.310	0.932
Proportion of Variance	0.73717	0.15416	0.10493	0.69313	0.18815	0.11597

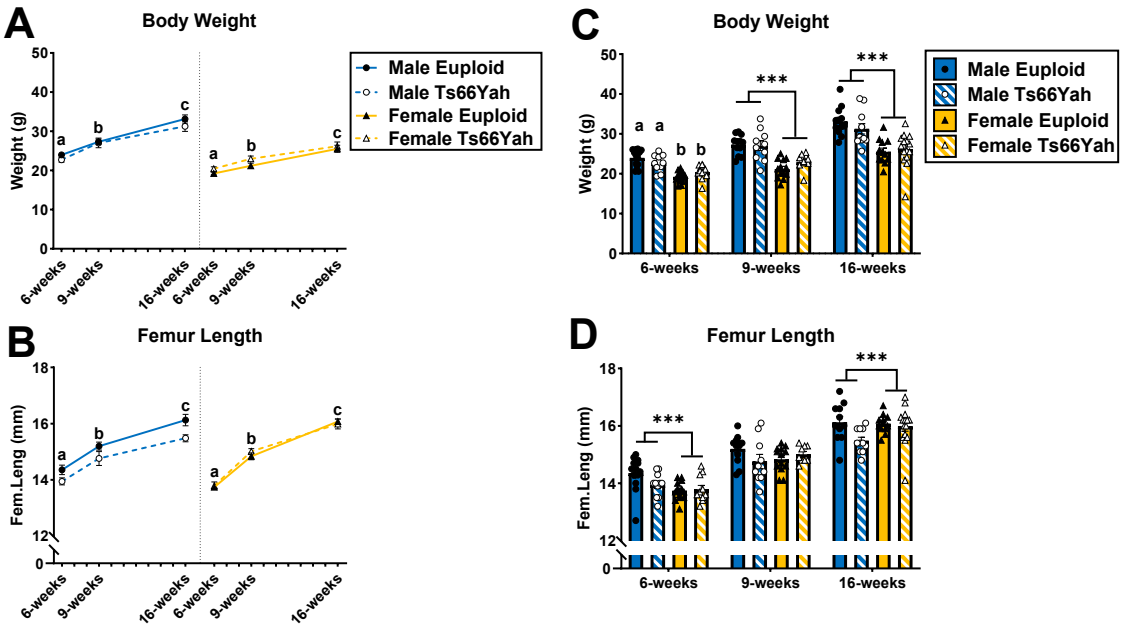

Supplemental Figure 1: **Body weight and femur lengths of 6-, 9-, and 16-week-old Ts66Yah mice.** Data are mean ± SEM. **A-B)** Different letters indicate $p < 0.05$ between ages as determined by two-way ANOVA and Tukey or Games-Howell *post hoc* analysis. **C-D)** Different letters indicate significant differences between groups as determined by Tukey or Games-Howell *post hoc* analysis of significant genotype × sex interaction. Asterisks indicate a sex effect as determined by two-way ANOVA. *** $p < 0.001$. 6 weeks: male euploid (n = 13), male Ts66Yah (n = 11), female euploid (n = 15 [body weight] or 13 [femur length]), female Ts66Yah (n = 12 [body weight] or 11 [femur length]); 9 weeks: male euploid (n = 12), male Ts66Yah (n = 10), female euploid (n = 13), female Ts66Yah (n = 9); 16 weeks: male euploid (n = 12 [body weight] or 11 [femur length]), male Ts66Yah (n = 11), female euploid (n = 12), female Ts66Yah (n = 15).

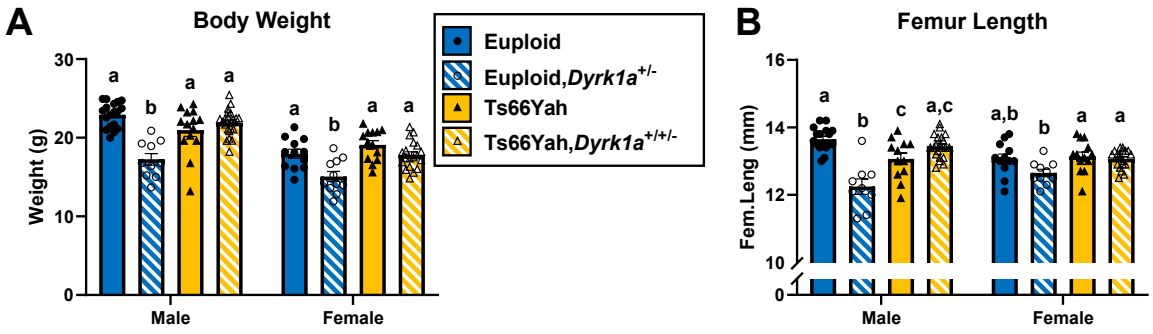

Supplemental Figure 2: **Body weight and femur lengths of postnatal day (P)36 Ts66Yah,Dyrk1a$^{+/+/-}$ mice.** Data are mean ± SEM. Different letters indicate $p < 0.05$ between groups as determined by Tukey or Games-Howell *post hoc* analysis of significant sex-stratified one-way ANOVA. Male mice: euploid (n = 18 [body weight] or 17 [femur length]); euploid,*Dyrk1a*$^{+/-}$ (n = 10 [body weight] or 9 [femur length]); Ts66Yah (n = 14 [body weight] or 12 [femur length]); Ts66Yah,*Dyrk1a*$^{+/+/-}$ (n = 22 [body weight] or 21 [femur length]). Female mice: euploid (n = 12); euploid,*Dyrk1a*$^{+/-}$ (n = 11 [body weight] or 10 [femur length]); Ts66Yah (n = 13); Ts66ah,*Dyrk1a*$^{+/+/-}$ (n = 19).

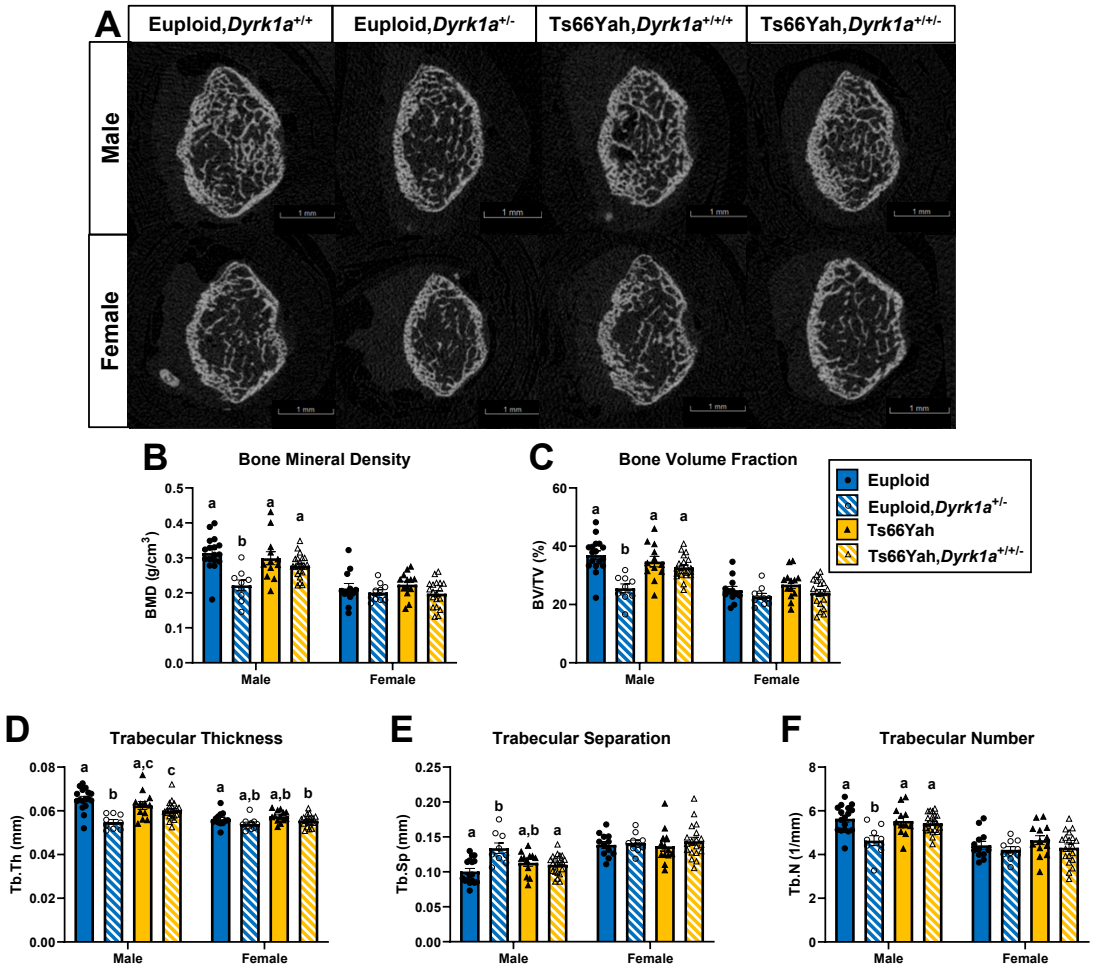

Supplemental Figure 3: **Trabecular bone parameters for P36 Ts66Yah,*Dyrk1a*$^{+/+/-}$ mice. A)** Representative images of trabecular bone taken halfway through the 1mm trabecular region as determined by finding the animal with the closest average distance away from the mean of each trabecular parameter. **B-F)** Data are mean ± SEM. Different letters indicate $p < 0.05$ between groups as determined by Tukey or Games-Howell *post hoc* analysis of significant sex-stratified one-way ANOVA. Male mice: euploid (n = 17); euploid,Dyrk1a$^{+/-}$ (n = 9); Ts66Yah (n = 12); Ts66Yah,Dyrk1a$^{+/+/-}$ (n = 21). Female mice: euploid (n = 12); euploid,Dyrk1a$^{+/-}$ (n = 10); Ts66Yah (n = 13); Ts66ah,Dyrk1a$^{+/+/-}$ (n = 19).

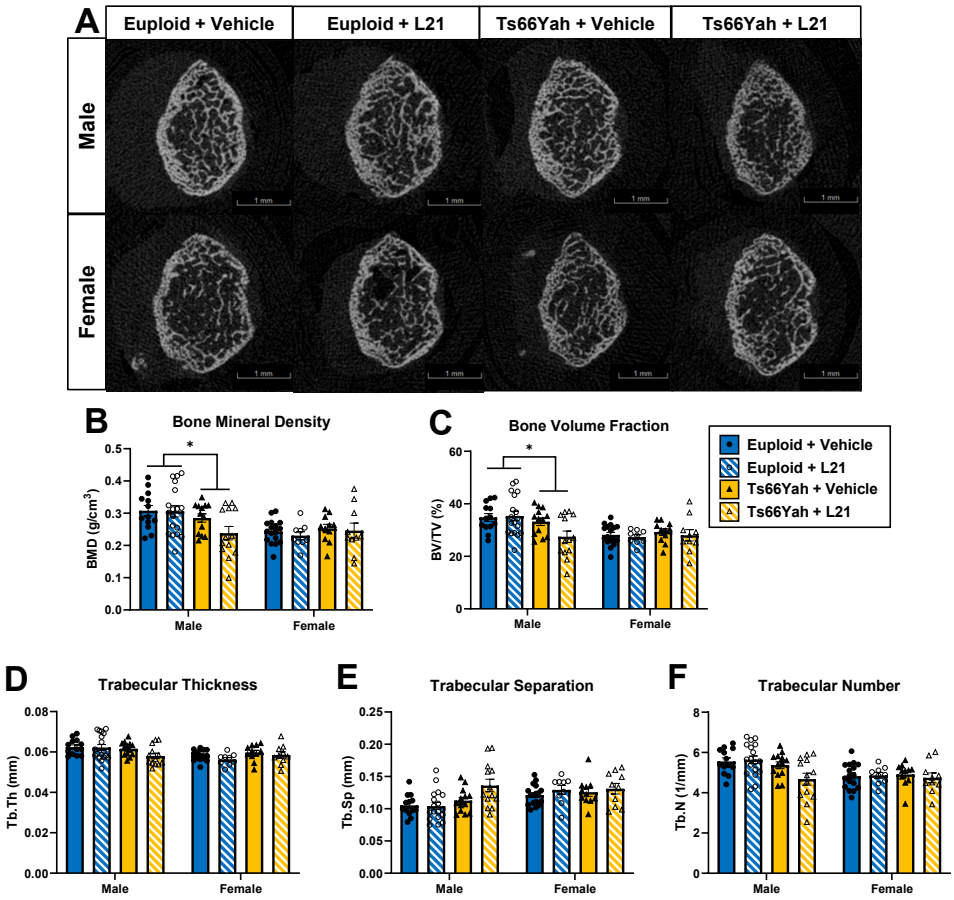

Supplemental Figure 4: **Trabecular bone parameters for Leucettinib-21-treated Ts66Yah mice. A)** Representative images of trabecular bone taken halfway way through the 1mm trabecular region as determined by finding the animal with the closest average distance away from the mean of each trabecular parameter. **B-F)** Data are mean ± SEM. Asterisks indicate a treatment or genotype effect as determined by sex-stratified two-way ANOVA. * $p < 0.05$. Male mice: vehicle-treated euploid (n = 13), L21-treated euploid (n = 18), vehicle-treated Ts66Yah (n = 13), L21-treated Ts66Yah (n = 13). Female mice: vehicle-treated euploid (n = 17), L21-treated euploid (n = 9), vehicle-treated Ts66Yah (n = 11), L21-treated Ts66Yah (n = 10).

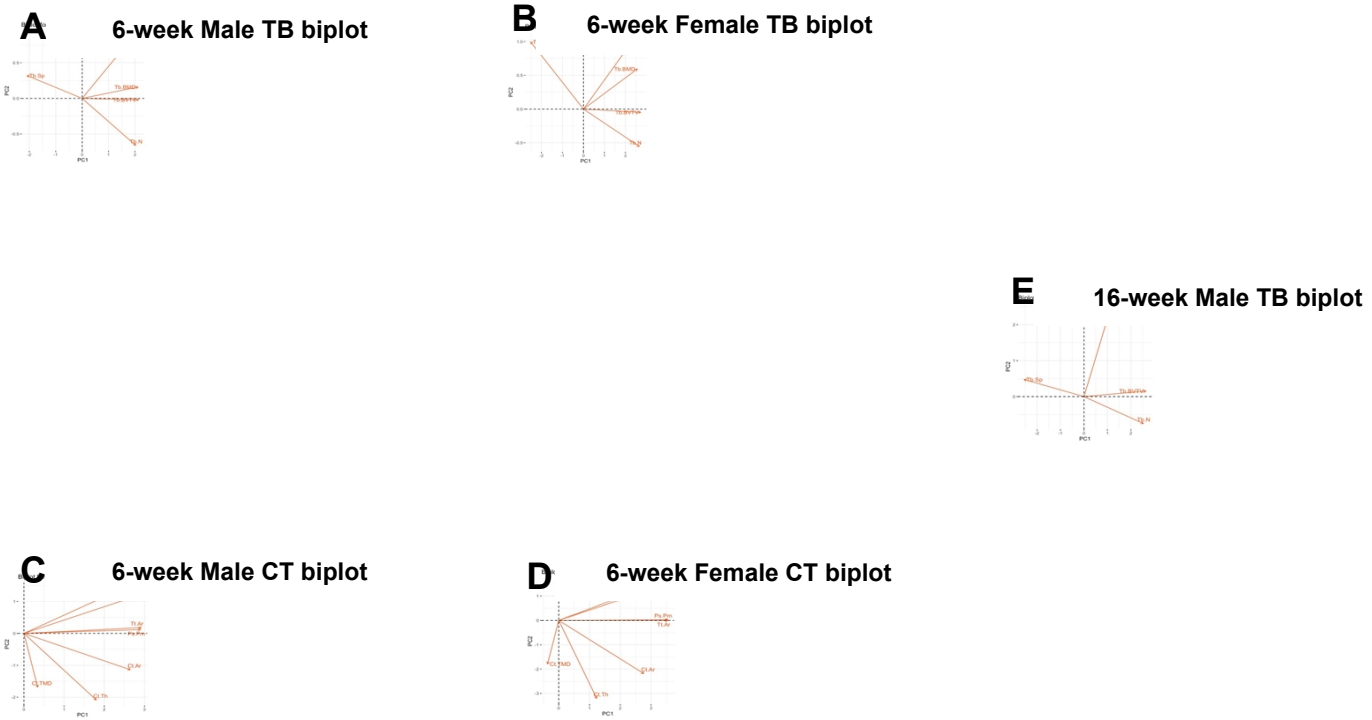

Supplemental Figure 5: **Principal component analysis biplots for trabecular (TB) and cortical (CT) parameters of Ts65Dn and Ts66Yah mice.** Six-week male and female Ts65Dn data from euploid littermates and Ts65Dn mice lacking OSX-cre (THOMAS *et al.* 2021). Sixteen-week male Ts65Dn data from (BLAZEK *et al.* 2011). See Supplemental Table 3 for PCA results.

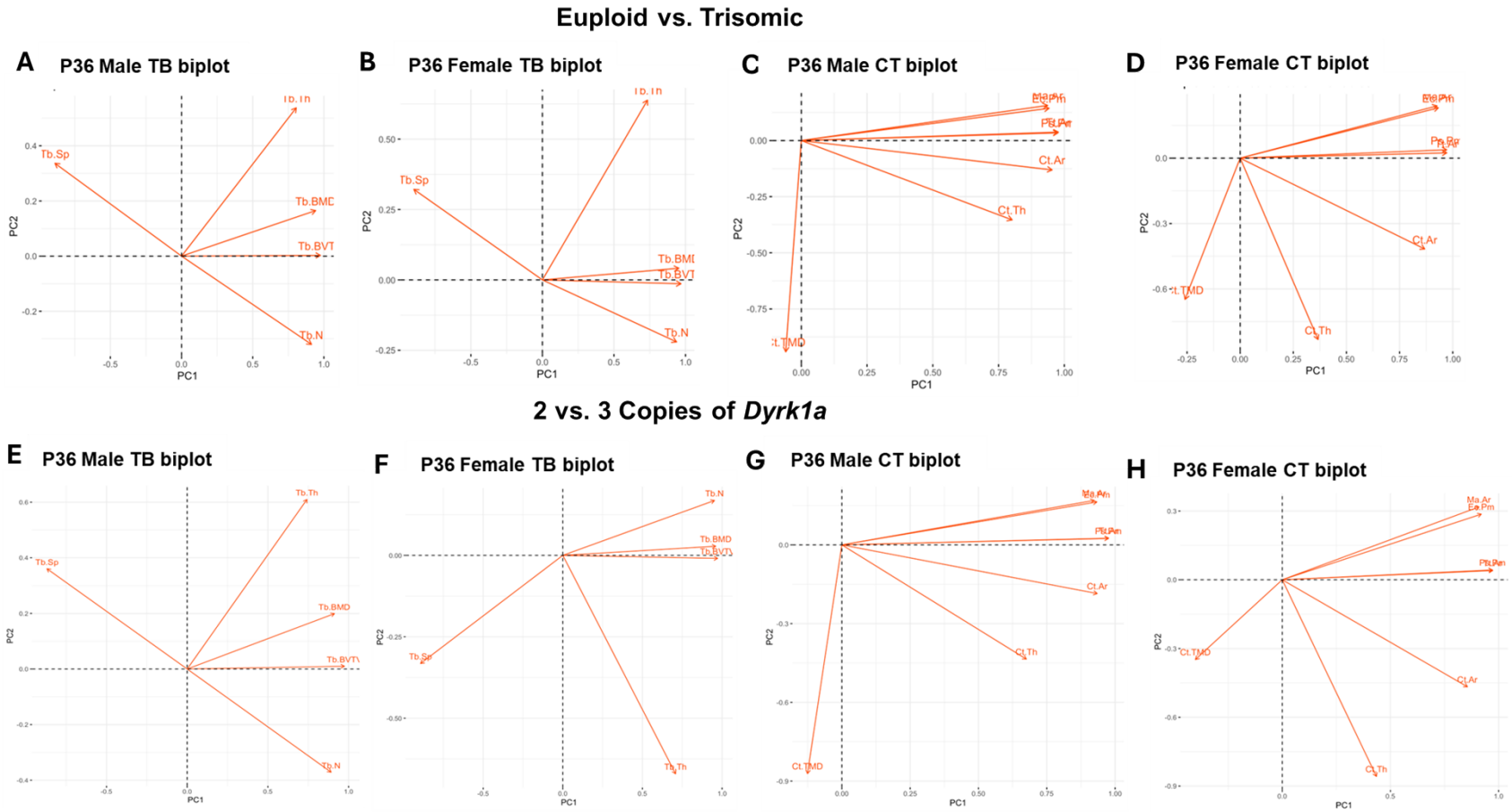

Supplemental Figure 6: **Principal component analysis biplots for trabecular (TB) and cortical (CT) parameters of Ts65Dn, Ts66Yah, and germline reduction of *Dyrk1a* copy number mice.** P36 male and female Ts65Dn data from (LACOMBE *et al.* 2024). See Supplemental Table 4 for PCA results.